



Universidad  
Carlos III de Madrid

BIOENGINEERING AND AEROSPACE ENGINEERING  
DEPARTMENT

# **FEASIBILITY STUDY FOR BRAIN PERFUSION ANALYSIS USING CHANGES OF $F_{iO_2}$ (INSPIRED OXYGEN PERCENTAGE) AND MAGNETIC RESONANCE IMAGING**

Final bachelor thesis

**Author: Adrián Romanillos Botella**

**Supervisors: Manuel Desco Menendez**

**Cristina Chavarrías Navas**

*Reading date: 14th July 2014*

# Acknowledgements

Firstly, I would like to thank my family all the support they have offered me during these intense four years, even though I have been absent from home. They strongly encouraged me to start this adventure four years ago and without their outstanding backing I would not be able to finish this bachelor degree. All I have become during my whole life is due to them.

I would also like to personally thank Cristina Chavarrías for their guidance and support during the development of the experiments, and has also helped me to refine my thesis. Thank you for all you have showed me about those topics I really love and for your patient during all this time. A special thank you to my supervisor Dr. Manuel Desco, because he offered me this project knowing my profile and initial intentions, and he trust on me to carry it out. This thesis would not have been possible without these people and their tremendous knowledge. Moreover, thank to those people who have offered me their selfless help in some aspects of the project, especially to my teacher Jorge Ripoll.

Finally I would want to dedicate some words to those teachers who really encourage me to follow this pathway and go further, and also to those friends on both sides of the Mediterranean Sea who have shared with me all my joys, failures, misfortunes, successes and defeats.

## Abstract

The term *perfusion* is usually employed to describe the process of nutritive delivery of arterial blood to tissues. In the case of the brain, perfusion is especially a crucial factor, since the intake of glucose and oxygen in this organ is continuous due to its extremely high activity and lack of reserves. Moreover, it is altered in many disorders, diseases and injuries, so it should be tightly controlled in order to ensure the proper functioning of the body. As previously mentioned, one of the most important parameters regarding perfusion is the level of oxygen that arrives to the tissue. The general term to describe oxygenation degree is the blood saturation,  $SpO_2$ , which is defined as the ratio between the oxygenated carrier, oxyhemoglobin, and the total amount of hemoglobin present in the bloodstream.

Due to its importance in diagnosis, cerebral perfusion has been studied by means of several techniques, such as MRI and CT. However, in both cases perfusion is assessed using an external contrast agent, such as Gadolinium or iodinated compounds. By introducing external contrast agents, images do not rely upon intrinsic properties of the tissue, and injection process increases medical expenses, patient discomfort, and may involve certain risks.

Therefore, this project has been developed in order to analyze the feasibility of a novel approach to assess perfusion, using the own blood as an endogenous contrast agent, using magnetic resonance imaging (MRI). The approach relies on how abrupt changes in saturation affect to the mean intensity of certain zones in the MRI image. BOLD is a classical technique that follows a similar procedure, but it only studies differential perfusion changes during neuronal activation, instead of analyzing large changes over time.  $SpO_2$  alterations are achieved by modifying the fraction of oxygen inhaled, or  $FiO_2$ . For that purpose, a gas mixer device supplies different mixtures of  $O_2$  and  $N_2$ , with 0% and 100% oxygen content, respectively. Both mixtures are alternated in order to achieve an abrupt fall in saturation levels and a further recovery of those values, generating concatenated downwards and upwards slope in the saturation curve. Saturation values, which represent the input function to the system, are recorded using pulseoximeter devices. During those changes, image acquisition is performed in parallel, in order to record how mean intensity is affected in the image. Two different pulse sequences have been tested in the experiments, *Spin Echo Planar Imaging* (SE-EPI) and *Gradient Echo* (GE).

The results show a drop in the mean intensity values of the SE-EPI sequences, coinciding with the drop in the saturation curve registered by the pulseoximeters. No changes appeared with GE sequences.

Therefore, the project shows that under certain conditions, the own blood could act as an endogenous contrast agent for perfusion analysis using MRI, thus opening up a wide range of possibilities for the future.

# General Index

Abstract.....	3
1 Introduction and theoretical frame .....	7
1.1 Magnetic Resonance principles .....	7
1.1.1 Physical principles .....	7
1.1.1.1 Introduction .....	7
1.1.1.2 Physics.....	9
1.1.1.3 Precession .....	11
1.1.2 Signal detection.....	13
1.1.2.1 Excitation.....	13
1.1.2.2 Relaxation .....	14
1.1.3 Basic Instrumentation .....	16
1.1.4 Pulse sequences .....	17
1.1.5 Image acquisition .....	18
1.2 MRI applications: The brain .....	20
1.2.1 Cerebral vascular system .....	20
1.2.2 Cerebral blood flow.....	20
1.2.3 Cerebral perfusion .....	21
1.3 BOLD signal .....	21
2 Motivation and objectives .....	22
2.1 Motivation.....	22
2.2 Objectives.....	24
3 Materials and methods.....	25

3.1	Materials .....	25
3.1.1	MRI scanner and sequences .....	26
3.1.2	Coils .....	27
3.1.3	Gas mixer .....	28
3.1.4	Pulseoximeters.....	30
3.1.5	Labview program .....	33
3.2	Methods.....	35
3.2.1	General design .....	35
3.2.2	Pulseoximeters synchronization .....	39
3.2.3	Dead volume .....	40
3.2.4	Pulseoximeter curves .....	40
3.2.5	Image acquisition .....	41
3.2.6	Image processing .....	43
4	Results.....	44
4.1	Pulseoximeters synchronization .....	44
4.2	Dead volume .....	45
4.3	Pulseoximeter curve profile .....	46
4.4	Image acquisition.....	48
4.5	Image processing .....	49
5	Discussion and conclusions.....	55
5.1	General discussion .....	55
5.2	Future experiments and improvements.....	57
6	References .....	58

# 1 Introduction and theoretical frame

## 1.1 Magnetic Resonance principles

### 1.1.1 Physical principles

#### 1.1.1.1 Introduction

In the last century, several medical imaging techniques have been developed by scientists and engineers in order to achieve a better anatomical and patophysiological information about clinical disorders. As far as anatomy is concerned, Computed Tomography (CT) X rays-based procedures (for 3-D) and conventional radiography are the most widespread techniques in most clinical scenarios. This modality of medical imaging relies on the absorption of high energy photons (x-rays photons) by the different types of tissue, depending on their densities and atomic number (Z). On the other hand, regarding functionality and physiology, one of the preferred approaches is Nuclear Medicine. In Nuclear Medicine studies, the image is a map of the location of a radioactive compound, previously introduced into the patient in several ways, and followed along its pathway through the body. That radioactive compound is called 'radiotracer' and whilst it decays, it radiates (directly or indirectly) high-energy gamma photons, which are collected afterwards by the detector, which enables the location of the original place from which it had been emitted. Both kind of medical imaging techniques rely on very energetic photons and may cause damage to the tissues as it is ionizing radiation, which detaches of electrons from the atoms and may induce undesired chemical reactions.

Both X-rays and gamma rays are electromagnetic waves. The energy  $E$  of a photon with frequency  $f$  and wavelength is

$$E = h \times f = h \times \frac{\lambda}{c}$$

where  $h$  is the Planck's constant (  $h = 6.62606957 \times 10^{-34} \text{ m}^2 \text{ kg} / \text{s}$  ) and  $c$  (  $299.792.458 \text{ m/s}$  ) is the speed of light in vacuum.

The electromagnetic spectrum (Figure 1) shows the different kinds of radiation utilized for medical imaging applications.

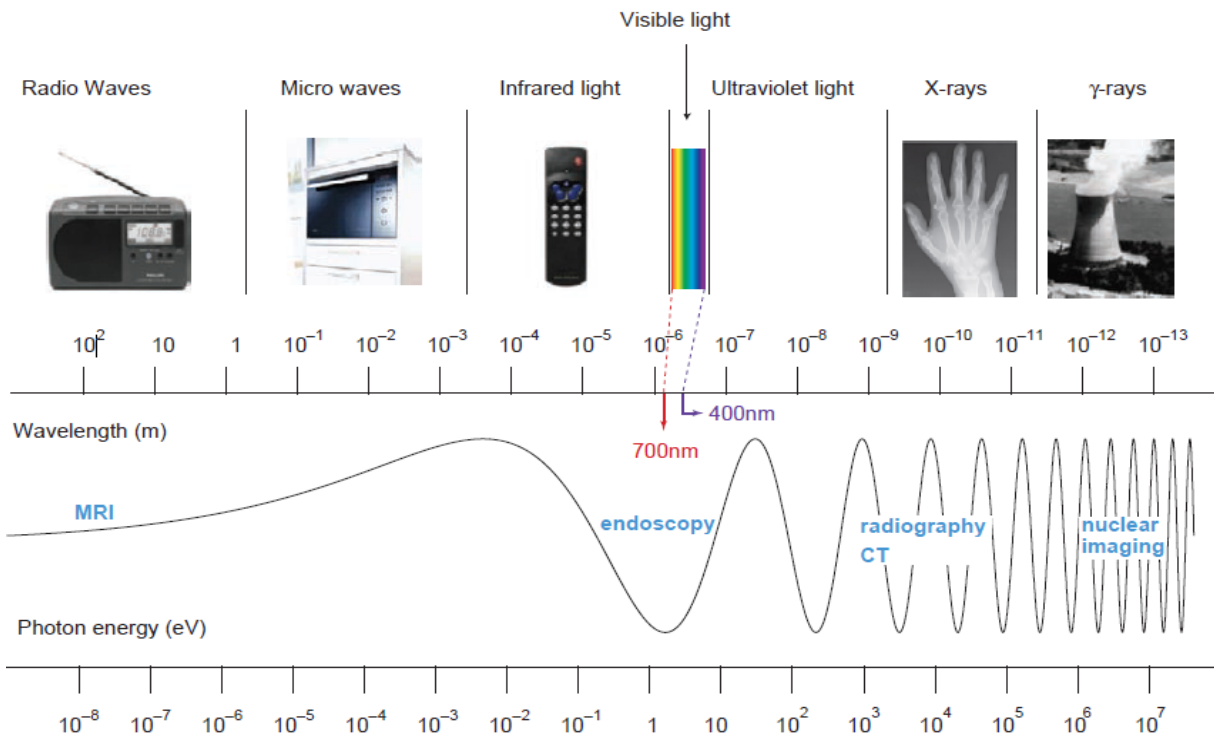


Figure 1 . Electromagnetic Spectrum ( P. Suetens 2009)

Unlike the two previously mentioned cases, Magnetic Resonance Imaging (MRI) does not make use of ionizing radiation, and the information content of the images depends on the material and its chemical environment. The type of energy which is irradiated into the sample in this modality is radiofrequency energy, as shown above (Figure 1). Therefore, MRI is a non-invasive technique, highly safe, accurate and reliable, and it does not produce harmful effects as ionizing radiation. It has become an indispensable widespread tool for prevention and diagnosis due to its high flexibility. Magnetic resonance imaging reveals fine details of anatomy and offers several contrast possibilities, since the image is generated according to certain parameters which could be easily modifiable in order to enhance different kinds of tissues. Accordingly, MRI has a great spatial resolution and excellent contrast in soft tissue, although it is a little less sensitive for detecting imaging probes [1].

Strictly speaking, MRI measures how the system recovers its initial value (relaxation) after the system has been disturbed (excitation) by electromagnetic radiation while it is under the effect of an intense magnetic field. Besides, magnetization and resonance involve many physical phenomena, which explain the full range of MRI possibilities and applications [2].



### 1.1.1.2 Physics

The physical property actually measured in MRI is known as nuclear magnetic resonance (NMR). NMR is a complicated process not easy to understand at the first glance, as it requires knowledge from different fields. For instance, the microscopic approximation is an easier approach that takes into account the contribution of a set of nuclei to explain the phenomenon classical physics, but cannot explain many aspects of the process. On the other hand, quantum mechanics approximation relies on the study of single nuclei but it is considerably more complex.

In fact, MR is based upon the interaction between an applied static magnetic field and a nucleus that possesses spin. The angular momentum linked to that nuclear spin is one of several intrinsic properties of subatomic particles (the nucleus, in the case of NMR) and varies for one element to another. Atoms are conformed by three fundamental particles: electrons, which are negatively charged; protons, which possess positive charge; and neutrons with no charge. Both protons and neutrons form the core of the atoms, known as the nucleus, whereas the electrons surround the nucleus. In fact, the number of protons, also known as atomic number  $Z$ , delimits the characteristics of the element, and two different elements cannot have the same atomic number. The number of protons plus the number of electrons is the mass number  $A$ , and same elements with different mass number are denominated isotopes. Finally, electrons do not contribute to the atomic weight, but determine the charge of the whole atom. Same elements with equal mass number but different number of electrons are called ions [3, 4].

Magnetic resonance, as mentioned above, relies on the intrinsic spin angular momentum of the nucleus. According to classical electromagnetism, the nucleus could be considered as constantly rotating about an axis with constant velocity, and the direction of rotation and the axis are considered perpendicular one to each other (Figure 2). However, the spin is quantized in nature and adopts a limited number of discrete values ( $I$ ) depending on the composition of the nucleus. If atomic number and mass number of the element are both even, the value of the spin is zero. Otherwise, the spin has a discrete value depending on if both numbers are odd, which means that the nucleus has an integral value for  $I$  (e.g., 1, 2, 3), or if it has an odd atomic weight, which means half-integral value for  $I$  (e.g., 1/2, 3/2, 5/2).

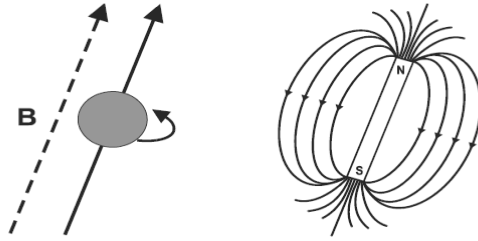


Figure 2. Nuclear spin. [4]

From classical electromagnetism, spin is interpreted as if the nucleus were rotating around its own axis, producing an angular momentum. Moreover, rotating charges produce a magnetic moment. Both moments are related by the gyromagnetic constant,  $\gamma = \frac{|\mu|}{|L|}$ , which is different for each element. Therefore, spin determines the intrinsic magnetic property that has a direct influence on magnetic resonance imaging. Table 1 shows different elements with its corresponding mass number, its natural abundance and its gyro magnetic constant. This parameter determines the feasibility of performing magnetic resonance experiments with them.

Element	Nuclear spin ( <i>I</i> )	Gyromagnetic constant (Mhz / T)	Natural abundance (%)
<b>1H</b>	1/2	42.58	~100
<b>2H</b>	1	6.53	0.015
<b>13C</b>	1/2	10.71	1.1
<b>12C</b>	0	-	99.8
<b>14N</b>	1	3.1	99.6
<b>23Na</b>	3/2	11.26	~100
<b>16O</b>	0	-	~100
<b>31P</b>	1/2	17.24	~100

Table 1. Spin values and other parameters of different elements

In order to perform magnetic resonance imaging, nuclei must contain an odd number of protons and/or neutrons. Most part of our body contains water, especially soft tissue. The biological abundance is lead by hydrogen ( $^1\text{H}$ : 63%), followed by oxygen ( $^{16}\text{O}$ : 26%) and carbon ( $^{13}\text{C}$ : 9.4%).  $^1\text{H}$  is thus the nucleus of choice for performing MRI, and that is the reason why MRI has excellent contrast in soft tissues, as they contain high levels of water and therefore hydrogen atoms which produce the desired phenomenon [4].

#### 1.1.1.3 Precession

Those properties and characteristics previously mentioned are required in order to achieve magnetic resonance signal and imaging. However, they are intrinsic properties that remain unaltered if no further action is exerted. Therefore, some external conditions must be performed in order to collect the information needed to create an image. From the classical physics perspective, all the nuclei are rotating in random orientations at equilibrium. Therefore, the contributions of all their spins cancel out among them and the net magnetization of the whole sample is zero, as shown in Figure 3.

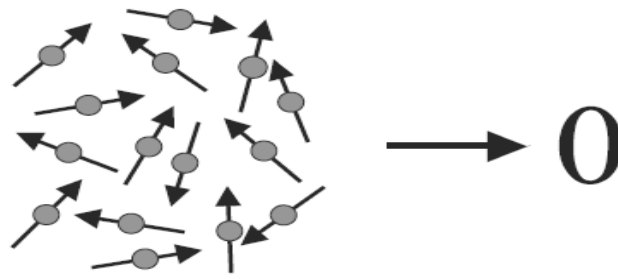


Figure 3. The vector sum of the spins is zero [4]

Notwithstanding, if the sample is placed under the influence of a magnetic field  $B_0$  the individual  $H^1$  protons begin to rotate in alignment with the magnetic field, although the protons are slightly tilted away from the axis of the magnetic field  $B_0$ . This phenomenon is known as precession. This precession undergoes at constant rate and occurs because of the interaction of the magnetic field with the spinning positive charge of the nucleus. The rate of precession is proportional to the strength of the magnetic field and its value is given by Larmor's frequency formula  $\omega_0 = 2\pi f_0 = \gamma B_0$  [1, 4, 5].

From a quantum mechanics perspective, spins must be quasi-aligned with the magnetic field in either parallel or anti-parallel configurations. The orientation and the corresponding energy levels depend on the spin number. There are more spins pointing towards the parallel direction (spin up) than towards the anti-parallel one (spin down), because parallel organization requires less energy (Figure 4). However, transitions happen between both states occur continuously in a dynamic equilibrium. The difference on energy between both states is given by the expression  $\Delta E = \frac{h}{2\pi} \gamma B_0$ , being  $h$  the Planck constant.

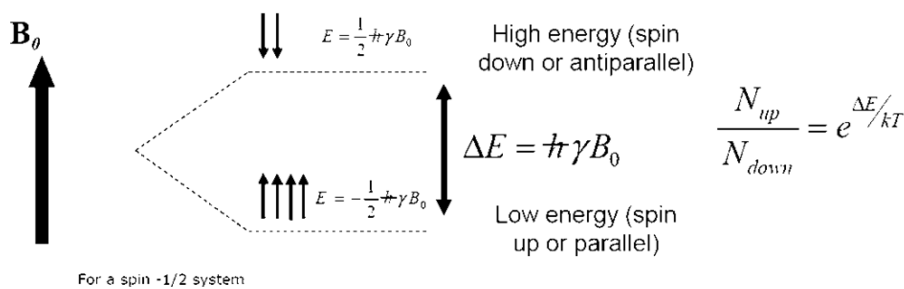


Figure 4. Difference in energy between opposite spin configurations

Due to this energy difference between states, the precession of many nuclei produces a net magnetization vector, due to the sum of all the individual magnetization vectors, which does not cancel out and points in the direction of  $B_0$ . The magnetization vector has two different components: a longitudinal one, in the direction of  $B_0$ , namely  $M_z$ , which predominates at resting state, and a transversal component in the perpendicular plane, namely  $M_{xy}$ , which is almost cancelled at resting state. The magnitude of the magnetization vector is given by  $|\vec{M}| = \frac{\gamma^2 \hbar^2 B_0 N_s}{4KT_s}$  being  $N_s$  the number of samples and  $T_s$  the temperature of the sample. The net magnetization vector usually points upwards since the majority of the components remain in the low-energy level [4]

### 1.1.2 Signal detection

#### 1.1.2.1 Excitation

The local equilibrium magnetization  $M$  is the difference between the aligned dipoles both parallel and anti-parallel, but it is not directly observable because it is several orders of magnitude weaker than  $B_0$ . Moreover, due to Faraday's Law, a static magnetic field does not produce any electrical signal that could be measured. Thus, the system must be somehow disturbed in order to be capable of producing signals which could be recorded. The disturbance is accomplished by a radio frequency pulse. According to Faraday's law, an oscillating RF current in a coil produces an oscillating magnetic field  $B_1$  perpendicular to  $B_0$ , which is applied to the sample. If the frequency of the perpendicular field differs from the Larmor frequency, the net magnetization vector  $M$  stays almost the same, except for a little wobble around  $B_0$ . However, if the frequency of the oscillating perpendicular field coincides with the Larmor frequency of the system, the resonance phenomenon occurs. Then the net magnetic field starts to wobble, drawing away of the initial vertical value, tracing a spiral during its trajectory. The vector is flipped down into the transversal component  $M_{xy}$ : this process is known as excitation (Figure 5). The angle that is turned is called flip angle, and is given by  $\theta = 2\pi\tau\gamma B_1$ , where  $\tau$  is the amount of time that the magnetic pulse  $B_1$  is applied. During this process, the longitudinal magnetization  $M_z$  in the vertical plane is reduced and it disappears with a flip angle of  $90^\circ$ , and the transversal component lies onto the XY horizontal plane. The flip angle, as shown in the expression, depends on the strength of the applied perpendicular field and the time the field is acting onto the sample.

Since the spiral pathway followed by the magnetization vector difficult the visualization of the flip angle and the tilt process, the frame of reference is usually changed as shown in

Figure 5 to another rotating one in which only the tilt component is visible, instead of the complete circular motion. The variations in  $M_{xy}$  can be measured by the radiofrequency coils. When the RF pulse is turned off, *relaxation* processes start and the longitudinal component is recovered, whilst the transversal is lost. These processes will cause variations which could also be measured, and in fact is the important source of information for the image formation, so it will be explained deeply in the following topic [2].

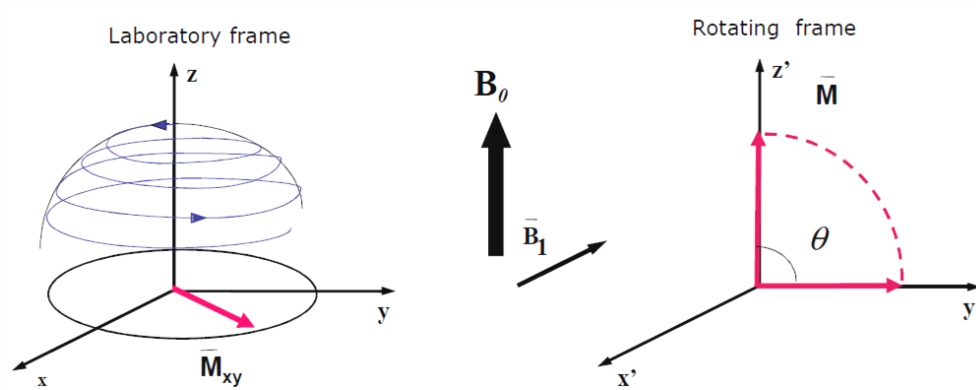


Figure 5. Framework reference[6]

### 1.1.2.2 Relaxation

Relaxation concerns the processes by which the system returns to its original, unexcited state. There are two kinds of relaxation processes: spin-lattice relaxation (recovery of the longitudinal component of magnetization) and spin-spin relaxation (loss of the transversal component of magnetization). Spin-spin relaxation occurs faster than spin-lattice relaxation (both kinds of relaxation are independent from each other). All the processes can be described by Bloch equations.

*Spin-lattice relaxation:* Energy is exchanged between excited nuclei and lattice. The process is characterized by a time constant  $T_1$ . The value of  $T_1$  is tissue-dependent because the efficient transfer of energy to the lattice depends on molecular motions (such as rotational, translational and vibrational). This is why solids have longer  $T_1$  values than solutions or viscous liquids, and these have longer values

than pure liquids.  $T_1$  values are also dependent on the magnetic field strength (because the total net magnetization vector is proportional to  $B_0$ ) and are normally defined for each kind of tissue and magnetic strength (usually 1.5 T), where lower  $T_1$  values mean that the magnetization is recovered faster. The differences in the  $T_1$  values can be translated into a  $T_1$  weighted image, since some tissues recover its initial transversal component faster.  $T_1$  weighted image exploits this fact by selecting a point in time where the values of the transversal component are wide different, as shown in Figure 6. At that time, tissue A would appear brighter in the final image.

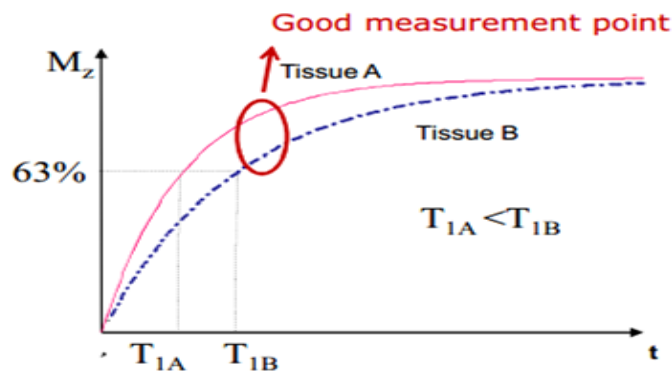


Figure 6. Transversal relaxation

*Spin-spin relaxation:* Interactions between spins create random local variations, which cause a gradual and random dephasing of spins in the transversal plane, causing a decrease in the transversal magnetization component (Figure 7.a). This process is characterized by the time constant  $T_2$ . Physical state of molecules and molecular size affects  $T_2$  as well as it affected  $T_1$ . Pure solids and large molecules present low  $T_2$  values while liquids present longer  $T_2$  values. These differences in  $T_2$  can be used to produce a  $T_2$  weighted image (Figure 7.c). Nevertheless, spin coherence is also affected by field inhomogeneities, so in many cases we need to correct the constant  $T_2$  to take into account those field inhomogeneities, obtaining a new constant called  $T_2^*$ , which is the one which measures the real rate of free induction decay (FID) (Figure 7.b). The free induction decay represents the loss of energy in the nuclei by emitting their own RF signal when perpendicular field  $B_1$  is arrested. Due to those inhomogeneities, and the interaction between nuclei, transversal magnetization vanishes much before the spin-lattice relaxation totally recovers the longitudinal component [1, 2, 4].

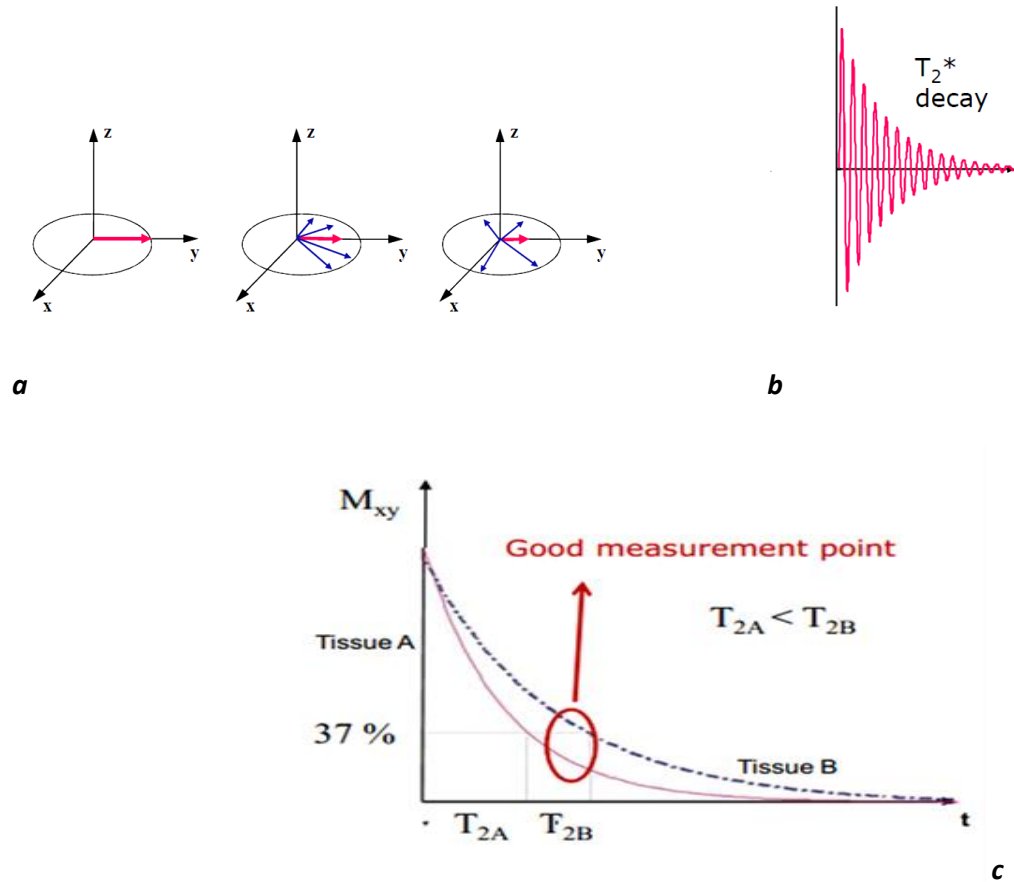


Figure 7. a) Spin dephasing b) FID c) Longitudinal relaxation

### 1.1.3 Basic Instrumentation

First of all, the samples are located under the influence of a strong magnetic field  $B_0$ . Afterwards, perpendicular magnetic pulses  $B_1$  at the Larmor frequency are applied through an RF coil, which can also act as the detector of the signal, which contains the information from the sample. Auxiliary magnetic field gradients are needed in order to spatially differentiate our sample -to encode the sample space into a pixel matrix-, and electronics and software to process the MR signal.



*Magnetic field  $B_0$ :* It is a magnetic field characterized by its high strength (0.5-3 Tesla for clinical purposes, 7-11.7 Tesla for preclinical research), static, and more or less homogeneous, although field inhomogeneities might appear and need to be compensated for. In order to produce the magnetic field  $B_0$  there are several solutions: resistive magnets, permanent and superconducting magnets. Nowadays, the latter configuration is the most effective, by using coils of superconducting wire (niobium-titanium alloy, for example). It works under cryogenic conditions in order to reduce resistance to almost zero, so the magnets are surrounded by liquid helium.

*Gradient coil systems:* They are a system of coils used to create spatial coding of the signal emitted from the region of interest, superimposing another magnetic field to the main field  $B_0$ . These coils are located inside the gantry and create gradients in any x, y, z directions, or combinations of them in any other direction.

*Radiofrequency coils:* they produce the excitation ( $B_1$ ) and the signal detection. They must be conveniently tuned and matched in order to optimize the image. There are two types: volume and surface coils. Volume coils offer a more uniform signal over the whole field of view, but lower signal to noise ratio (SNR) than surface coils. On the other hand, surface coils improve the latter parameter, but reducing signal homogeneity [7].

*Shielding:* Since the magnetic field in the magnetic resonance machine is so strong, it may cause problems in the region surrounding the magnet. A shielding is performed passively (metallic) or actively (outer superconducting coils whose field opposes that of the inner coil), causing the field to rapidly decrease out of the machine [8]

*Shimming:* It is a process performed in order to obtain a field as homogeneous as possible. It can be done passively, using ferromagnetic material, and/or using small coils to locally adjust the magnetic field (active shimming) [8, 9] .

#### 1.1.4 Pulse sequences

An MRI sequence is an ordered combination of RF pulses and magnetic field gradients designed to encode and acquire enough data to be able to reconstruct the image. Depending on the MRI sequence chosen, the number, type, position and duration of pulses will be different, and in this way the contrast in the final image will be determined:

*90° pulses:* they are used in order to flip the magnetization into the transversal plane. Since the evolution of the signal is what is recorded in MRI sequences, this pulse is always needed in order to produce signal. Nevertheless, the signal can also be obtained with lower angular pulses (75°, 60°...) although the strength of the signal would be lower.

*180° pulses:* they are used to reverse the effects of field inhomogeneities regarding dephasing processes, rephasing the spins in the opposite direction to produce an echo and allowing the acquisition of signals with a weight of  $T_2$  instead of  $T_2^*$  [4].

Echo generation is important since it adds important information which is not totally read with the FID. Depending on the type of sequence carried out, the echo is generated by the 180° pulse (Spin-echo) or by an additional gradient (Gradient-echo). We can define two parameters which should be taken into account in all the sequences; *Echo time (TE)*: It is the time between the 90° pulse and the reception of the echo; *Repetition time (TR)*: it is the time between two consecutive 90° pulses.

*Spin-echo sequences:* In these sequences, the 90° pulse generates a signal. When the signal is almost completely lost due to dephasing caused by field inhomogeneities and spin-spin interactions, a 180° pulse is applied pulse forcing the spins to rephase again, generating another signal, the echo. Since the inhomogeneities have been corrected, echo amplitudes decay with  $T_2$ .

*Gradient-echo sequences:* these sequences use a magnetic field gradient to induce the formation of an echo. An initial magnetic field gradient pulse produces a dephasing of the spins, and then an echo is produced by applying a reverse gradient pulse. This technique is faster than spin-echo, but has several drawbacks: it does not correct for field inhomogeneities, so the decay of the signal will be given by  $T_2^*$  and not by  $T_2$ . The flip angle would be smaller than in spin echo sequences and this plays an important role in the image contrast [4, 5].

### 1.1.5 Image acquisition

Image acquisition requires several steps in order to select the field of view, the contrast source ( $T_1$ ,  $T_2$ ) and the acquisition time. Some of the steps involved are difficult to understand and they are out of the scope of the project. However, it is important to remark that the MRI scanner acts as a physical Fourier Transform, registering spatial frequency information from the sample, filling which is known as the K-

space. The system scans every row of the k-space filling it with the information encoded by the gradient coils depending on the several parameters:

*Slice selection (z-gradient):* In order to select which slice of the patient we want to acquire, we need to apply a gradient with the gradient coils mentioned above in order to vary the total magnetic field and frequency of precessions as a function of position. This gradient should simultaneously with the initial 90° pulse and then with any  $B_1$  pulse, in order to acquire the signal from the very same slice. The bandwidth of the pulse and its amplitude determine exactly the slice which we will excite and the slice thickness. The gradient can be created in any direction, allowing us to acquire slices with any orientation.

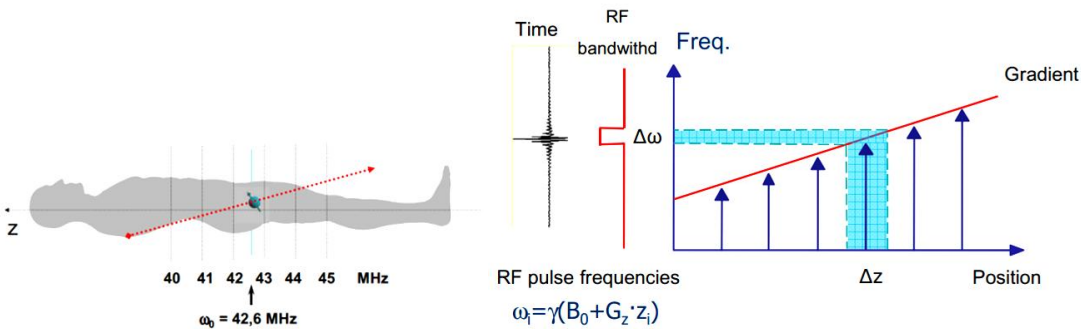


Figure 8. Slice thickness selection

*Physics of Fourier encoding:* When a gradient is turned on, some spins accelerate their precession rates whilst others delay it, causing dephasing. When the gradient is turned off, the spins recover the original precession frequency, but are still dephased following a sinusoidal pattern. From that we can obtain the weight of one term of the k-space.

*Phase encoding (y-gradient):* It consists in the repetition of the former process many times, by applying gradient pulses of different amplitude, allowing acquiring the weights of all the lines of the k-space. Phase encoding gradient should be performed before the readout.

*Frequency encoding (x-gradient):* The physical principle is the same as in the phase encoding processes. Now, we apply a cumulative dephasing during the signal readout, which is produced by a gradient pulse and its inverse one. This allows reading all the frequencies corresponding to one line of the k-space

(which was previously selected by the application of the phase encoding gradient). It should be applied simultaneously with the echo reception [4].

## **1.2 MRI applications: The brain**

As mentioned previously, MRI has both high spatial and contrast resolution for soft tissue. Hence, since brain is almost completely composed by soft tissue and fluid, it is the preferred imaging modality in neurology, being able to easily discriminate several disorders, as tumor or hemorrhage.

### **1.2.1 Cerebral vascular system**

Cerebral blood flow (CBF) is in charge of the delivery of glucose and oxygen to the different brain structures. Local blood flow might vary in different scenarios regarding brain activation or disease states. For instance, during a conversation, parts of the brain activated during speaking and listening induce changes in their respective local CBF. The vascular system that supplies blood to the brain is organized into several scales, which span a size range of three orders of magnitude, from the major artery (about 1 cm diameter) to the diameter of a capillary (10  $\mu\text{m}$ ). The major structure that supplies blood to the brain is the Circle of Willis, which contains the anterior and posterior circulation, composed by several arteries, such as the internal carotid arteries or the vertebral arteries respectively. However, we are going to focus more in detail on the microscopic capillaries which deliver oxygen and nutrients directly to the tissue [5, 10].

### **1.2.2 Cerebral blood flow**

In an adult, normal CBF is typically 750 ml per minute, and is tightly regulated to control the brain metabolism demand. High levels of CBF increases intracranial pressure, which could damage or compress tissue, and low levels produced by ischemia undergo tissue and cell death since not enough oxygen and glucose are delivered [19]. Therefore, it is important to control the parameters related with CBF, especially in patients who have already suffered from some cardiovascular or cerebral injury. CBF depends upon features such as blood viscosity, regulation of vessels diameter, and the net pressure of the flow of blood into the brain, known as cerebral perfusion. CBF is defined as the ratio between the

cerebral perfusion pressure (CPP) and the cerebrovascular resistance (CVR):  $CBF=CPP/CVR$ . Cerebrovascular resistance is controlled by several parameters, such as metabolism and pressure auto regulation, neural activity and chemical control (saturation) [5, 11].

### 1.2.3 Cerebral perfusion

Cerebral perfusion pressure (CPP) is defined as the pressure gradient causing cerebral blood flow through the brain structures. The term *perfusion* is usually employed to describe the process of nutritive delivery of arterial blood to tissues. It is an important factor since it involves factors as cerebral flow, cerebral volume, or blood velocity [5]. Moreover, it is altered in many disorders, diseases and injuries.

## 1.3 BOLD signal

The Blood Oxygenation Level Dependent (BOLD) effect is the basis for some studies related with cerebral perfusion using MRI. The fact that the change in the blood oxygenation originates a measurable effect on the magnetic resonance signal of the target tissue was discovered by Ogawa et al. in a rat-model [12]. They found out that the signal around veins decreased when the amount of oxygen inhaled was reduced, and the normal value was recovered when oxygen returned to the usual level. The oxygen sensitivity in MRI signal was discovered previously in several studies, which showed that the relaxation time  $T_2$  depends enormously on the oxygenation of the hemoglobin [13]. The BOLD effect is most evident with Gradient echo sequences (GRE), indicating that the effect is related to an increase of a local value of  $T_2^*$ , instead of  $T_2$ , since in gradient echo sequences no  $180^\circ$  pulses are applied and therefore field inhomogeneities are not corrected. Ogawa and his team suggest that the effect was due mainly to the alteration of the magnetic susceptibility of blood, similar to the effect of contrast agents, but in a weaker form. However, the important fact is that blood susceptibility could be considered as an intrinsic property, unlike external contrast agents. Others studies support this as the cause of BOLD effect, concretely MR signal decreased in an ischemia model, and it was attributed to a reduction of  $T_2^*$  by decreasing oxygen blood saturation. Moreover, Kwong and co-workers reported that brain activation induces a signal increase, indicating that the  $T_2^*$  had increased, suggesting that brain activation increases blood oxygenation at a higher rate than neurons were demanding it [14]. Several other groups also studied the same phenomenon that year [15-17].

This fact is due mostly to the effect of deoxyhemoglobin. Oxyhemoglobin is diamagnetic, so its magnetic field contribution is very weak. However, deoxyhemoglobin is paramagnetic, so its effect creates an additional magnetic field that is aligned with the external magnetic field. Therefore, the high concentrations of deoxyhemoglobin in low-oxygenated blood induce a change in the magnetic resonance signal recorded. Besides, under strong magnetic fields, Spin Echo sequences are frequently used because they lead to a better localization of BOLD signal, since the most part of the signal come from capillaries and micro vessels [18, 19].

Therefore, the BOLD effect appears because of two main reasons: (1) not oxygenated hemoglobin (deoxyhemoglobin) produces magnetic field fluctuations around blood vessels that decrease MR signal, and (2) brain activation is characterized by an increase in blood flow but not a commensurate increase in the oxygen consumption, thus leading to a drop in deoxyhemoglobin concentration [5].

## **2 Motivation and objectives**

### **2.1 Motivation**

A good quantification of cerebral perfusion may be extremely useful in the diagnosis of many cerebrovascular problems, such as stroke or ischemia. Moreover, for those who have already suffered those kinds of disorders, a post-injury control is even more important, in order to avoid future derived problems. One of those parameters shows the degree of oxygenated blood that arrives to the tissue, which is the oxygen saturation, or SpO<sub>2</sub>. Erythrocytes in the blood are the responsible of carrying up oxygen and transporting it through the whole body with the help of a carrier molecule called hemoglobin. There are two types of hemoglobin depending on the amount of oxygen which is attached to the molecule: oxygenated hemoglobin, known as oxyhemoglobin, and not oxygenated hemoglobin, or deoxyhemoglobin. The ratio between oxygenated carrier and the total amount of hemoglobin actually represents oxygen saturation in blood. SpO<sub>2</sub> is a crucial factor since the brain is always consuming oxygen due to its high activity, so it needs to be properly irrigated by blood. Otherwise, levels of oxygen decreases and tissue structures are not capable to carry out their normal metabolic activities. This is the reason why measuring local oxygen saturation helps to quantify cerebral perfusion in brain regions, which might help to study the disorders and injuries mentioned before, as well as the effectiveness of any treatment already performed [20, 21].

In fact, several functional imaging techniques try to deal with this phenomenon, as MRI and CT. MRI is a very attractive method in this area it relies directly on intrinsic properties of the tissue, instead of depending upon external features. In MRI, cerebral perfusion is studied mostly by the action of a contrast agent, normally Gadolinium, which produces a change of the signal in the vessels that allows clear visualization of the vessel map. However, by introducing a contrast agent the image does not rely anymore completely upon intrinsic properties of the tissue[22]. Moreover, the use of any external contrast agents increases the medical expenses during the procedure and requires an injection to the patient, increasing their discomfort, and also it may involve certain nephritic and dermatological risks which must be avoided whenever possible. On the other hand, x-rays based technologies are also utilized to determine some perfusion features by using iodinated contrast, so the problems mentioned before remains in this case. In addition, x-rays produce ionization, damaging somehow the tissue they penetrate, so it is even a worse approach compared with the previous case. For all those reasons, it is important to find out some feature which allows the study of cerebral perfusion avoiding the use of Gadolinium or any other external agent.

On the other hand, BOLD procedure is mainly devoted to functionally study regional brain activations, where the changes in perfusion are very small, and several statistical procedures should be performed in order to detect those minimal changes in intensity of the region of interest. This technique has not been used to detect high perfusion changes in broad areas of the brain, because it is a differential approach in which only little variations are measured in order to distinguish thoroughly neuronal activation, which does not imply large changes in perfusion.

Therefore, the main idea behind this work is to produce hemoglobin saturation changes in order to analyze how the own blood could play the role of an endogenous contrast agent. Saturation is usually a very stable parameter under no pathologic conditions, so studies regarding low saturation levels require some external action in order to decrease them. Saturation levels would decrease under two main circumstances: when oxygen is available but it has not been taken properly by hemoglobin (affinity problems), or when oxygen levels have abruptly decreased. Thus, the easiest way to lower oxygen saturation in the blood stream is changing the fraction of oxygen inhaled, or  $FiO_2$ . Abrupt variations are required, similarly as contrast agents are introduced into the body, in order to analyze whether those sudden sharp in  $FiO_2$  are translated into further changes in intensity of the image due to deoxyhemoglobin concentration. This is actually the main hypothesis of the work, and to our

knowledge, there are no previous attempts to use this mechanism to assess brain perfusion neither in humans nor in animal models.

## 2.2 Objectives

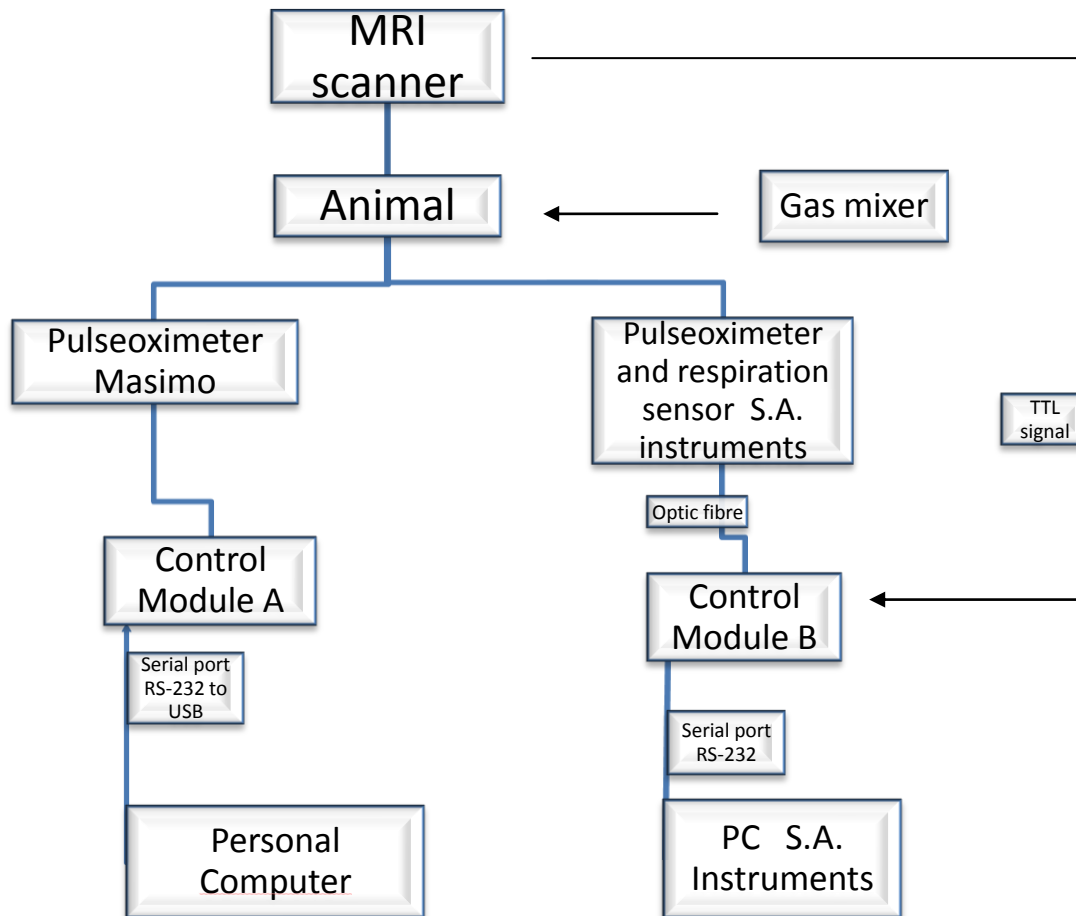
The general objective of the project is to analyze the feasibility of a novel approach to assess perfusion, using the own blood as an endogenous contrast agent, using an animal model. The approach is based on the effect of change in saturation over the BOLD signal on the brain. The specific goals of the project can be subdivided as follows:

- To study the possibility of sharply decreasing blood saturation by introducing abrupt changes in the fraction of oxygen ( $F_{iO_2}$ ) inhaled by the animal.
- To analyze the performance of several pulseoximeter devices in order to elucidate the degree of accuracy that can be obtained during the experimental procedures.
- To be able to detect changes in MRI BOLD signal in the images due to the application of those changes through the use of dynamic sequences.
- To evaluate the effects on BOLD the signal produced by drop and rise edges of the input signal ( $SpO_2$ ).
- To analyze the delay in both signals and determine the effect of the equipment, the system configuration and the animal physiology on that delay.



### 3 Materials and methods

#### 3.1 Materials



The scheme above represents an overview of the equipment and connections in the experiments. The subject under study, in our case a rat, was introduced in the scanner, and in order to proceed with the image acquisition, a surface cranial coil was used to receive the information, and a volume coil to transmit the excitation signal. Besides, the vital signs of the animal were controlled at every moment by several devices, such as two pulseoximeters and a respiration sensor. Both apparatus had their own control module to receive and record the information measured. The control module was connected to *S.A. Instruments* sensors via optic fibre, and in turn the control module was connected to the computer

by using a regular RS -232 serial port connection. In addition, a TTL trigger signal from the MRI scanner was also recorded in order to detect when the signal acquisition actually begins. This signal was directly connected to the control module B, and afterwards, to the computer, being recorded as an event together with the rest of the signals acquired from the animal. In order to facilitate the procedure, a LED was connected to the trigger in order to visually assess its state (high or low). On the other hand, the *Masimo pulseoximeter* was connected by a serial port RS-232-to-USB special adaptor, and its data were recorded by another personal computer.

### 3.1.1 MRI scanner and sequences



Figure 9. MRI scanner

The MRI scanner is a *BioSpec 70/20 USR (ultra shielding)* 7 Tesla from BRUKER manufacturer. It contains a superconductor magnet refrigerated by liquid helium, in order to achieve superconductivity. The black-yellow line on the floor indicates the perimeter of the area where the field is above 5 Gauss, and no magnetic objects should be introduced in that area. The scanner includes its own software (ParaVision) for controlling acquisition parameters and its routines are modifiable in order to fulfil the requirements for every experiment.

Two dynamic sequences were tested in order to get BOLD contrast, a spin echo EPI (Echo Planar Imaging) and a gradient echo FLASH (Fast Low Angle Shot). The particular parameters of each sequence will be explained in the experiment discussion.

### 3.1.2 Coils

For the experiments carried out during the study, two kinds of coils (both of *BRUKER*) have been used, according to their main function and characteristics. The volume coil is placed inside the gantry, surrounding the sample. Volume coils offer more homogeneous signal but with lower SNR. However, a good point regarding volume coils is their ability of working either in emitting or receiving mode. For the purpose of the experiments, volume coil worked as emitter, and must be coupled and tuned to the specific resonance frequency. This task is accomplishing by moving two rods that change capacitors inside the coil (figure 10).



Figure 10. Volume coil

On the other hand, since the target area under study is well delimited, a brain- surface coil was used for receiving the signal, due to its suitable shape for direct location onto the rat's head. The closer proximity of surface coils to the sample improves signal to noise ratio in reception. This surface coil contains four arrays elements, in order to further improve the signal received from the field of view (figure 11).

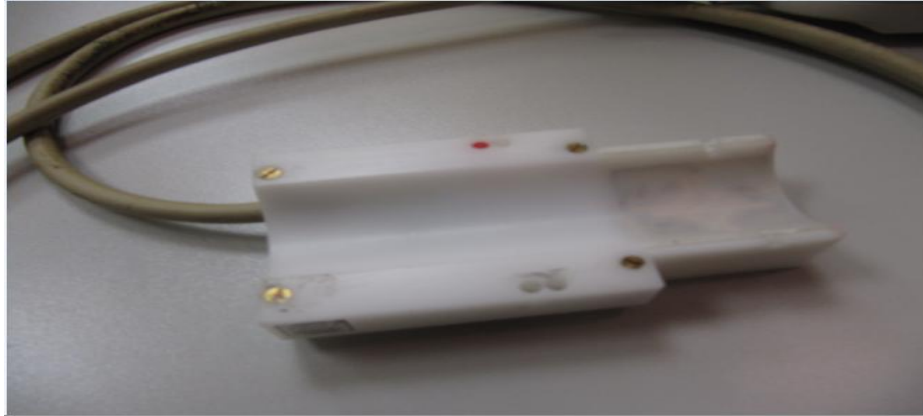


Figure 11. Surface coil

### 3.1.3 Gas mixer

The gas mixer is an important device in our setting since it is used for changing the percentage of oxygen inhaled by the animal during the experimental procedures.



Figure 12. Front view of the mixer

The device is a GSM-3 model manufactured by the company CWE, Inc. It offers two use possibilities. By moving upwards or downwards the left uppermost switch we select how the user controls the device; upwards sets a manual control while downwards allows the user to control the device from a computer. In the manual mode, the user is able to change the parameters directly on the screen with the console

knobs. The set of parameters chosen by the user defines a certain sequence, which defines the own features of a mixture. Each sequence is composed by three gases of the mixture, the percentage of each one, and the flow of the mixture (ml per minute). Several different sequences can be stored in the memory of the device for future applications by turning the two wheels located at the lower part of the device (stored mixture). Next to the knobs there is a white button used to launch the sequence and execute it, and a red button devoted to stop the flow whenever needed. In the screen the percentage of each gas and the total mixture flow are displayed. However, the device is usually controlled in remote mode, since it does not require direct manual interaction with the machine. A C-language code (supplementary material) has been developed in order to control the mixture composition and flow from the computer. The gas mixer is connected to the computer via RS-232 serial port (Figure 13). The program can be run from a shell through a command line with the appropriate arguments for the correct functioning of the complete system. The arguments needed are the switch mode (ON/OFF), the chosen channels (not important in remote mode), the three gases used with its corresponding percentage, and the total flow. The gases are coded with a certain number, whose values are displayed directly when no input arguments are introduced, and the program is executed. An example of command statement is (1 1 1 0 3 100 2 0 400). The first 1 represents the ON state; the second one represents the channel chosen; the third 1 is related to the gas introduced in the first gas inlet showed in the back view of the device, in this case air and 0%; the following two number represents the second gas inlet (in this case number 3 stands for oxygen) and its % within the mixture (100%). Similar thing occurs for the following two number (2, 0), for the third gas input and its percentage (2 for nitrogen at 0%). The last number, 400, represents the total flow of the mixture, in the example 400 ml /min. The numbers which correspond to each type of gas are defined previously in the program, included in the supplementary material. In order to stop the flow, the statement only needs a single 0 and no other input arguments are required. If the sum of all the fractions of the gases exceeds 100% or the number of input arguments is incorrect, errors are displayed.

Both inlet and outlet ports require 0.25" (6.35mm) O.D. semi-flexible tubing, which makes a press-fit connection. Tubes are connected to the embedded gas reservoirs by using valves which controls the input pressure of the gas itself, maintaining this value around 1 bar.



Figure 13. Rear view of the gas mixer

### 3.1.4 Pulseoximeters

Pulseoximeters are devices devoted to measure the saturation level of the hemoglobin carried out by red blood cells.. Saturation represents the proportion of oxygenated hemoglobin, or oxyhemoglobin, in relation to the levels of deoxygenated hemoglobin, or deoxyhemoglobin. Therefore, the functionality of the device is to discriminate between the two different kinds of hemoglobin in pulsatile blood, (that is, removing fixed components as tissue or venous blood), by means of the dissimilar light properties. Oxyhemoglobin and deoxyhemoglobin are two different molecules which absorb and reflect different light wavelength. Oxyhemoglobin absorbs infrared spectrum (900 nm) and transmits wavelengths corresponding to red spectrum (650 nm), passing through it. On the other hand, deoxyhemoglobin absorbs red spectrum and transmits wavelengths corresponding to infrared spectrum, as shown in the absorbance curve displayed in Figure 14.

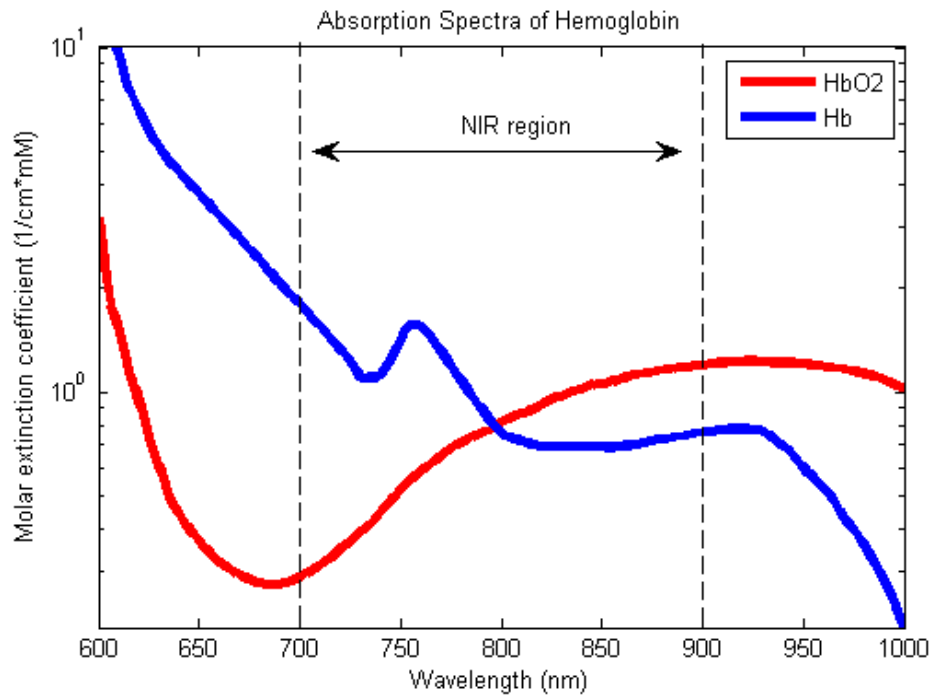


Figure 14. Blood absorption curve

Consequently, pulseoximeter must emit both kinds of wavelengths, red and infrared. Light is transmitted through a part of the body which contains a vascular pusatile component (usually a finger) and it is detected in the opposite side by a photodetector. The detector measures the amount of each light type received. Afterwards, the device calculates the total oxygen saturation in blood (SpO2) by figuring out the fraction of oxyhemoglobin over the whole amount of hemoglobin. Normal values in humans for SpO2 are around 98-99%.

Two different devices have been used in the experimental procedures:

*Masimo Radical -7*: Specially designed for humans, it measures saturation in a 0-100% range with  $\pm 2$ -3% range accuracy. It also contains different special clamps to measure other vital constants as pulse rate (PR), metahemoglobin (SpMet), Carboxihemoglobin (SpCO), Total hemoglobin (SpHb), total amount of oxygen (SpOC) and perfusion index (PI), among others. It is connected to the computer by a serial port, using a RS-232-to-USB adaptor. Moreover, the information is sent to the computer at a sampling rate of 1 Hz (one sample per second). Each second, the system sends a line with the time, SpO2, heart rate, perfusion index and, depending on the clamp used, the other parameters mentioned before. The port reading procedure is performed by a LABVIEW program designed within this project, which will be explained below.



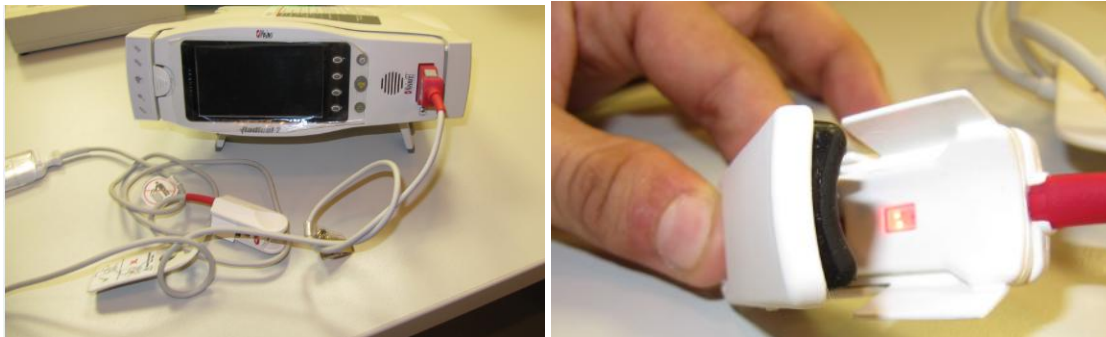
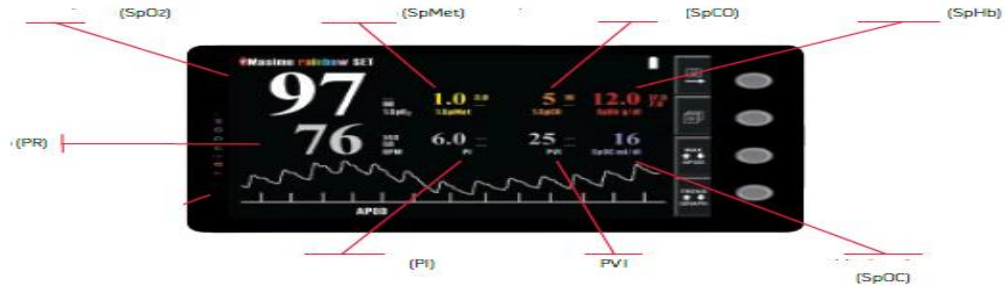


Figure 15. Masimo Radical-7

*S.A. Instruments pulseoximeter*: special for small animal and MRI compatible. In addition to oxygen saturation, the module measures the cardiac plethysmogram waveform, generates a plethysmogram gate, which measures pulse distension and the animal's heart rate. It uses fiber optic to transmit the information to the control module, and the control module is connected to the computer via serial port (RS-232). Its own software processes the information in the computer and displays the graphs obtained in the screen of the control PC.





Figure 16. S.A. Instruments device

### 3.1.5 Labview program

Masimo's pulseoximeter sends the information previously mentioned directly to the computer via RS-232 serial port. However, the device did not include any type of software to read the information. For that purpose, a LABVIEW software based program and its associated graphical user interface have been developed. The program basically reads the information present in the port selected by the user and displays it in the buffer, as long as no execution error is found. Moreover, in order to facilitate the posterior data processing using other software platforms, as Matlab or Excel, the information is written continuously into txt files previously created by the user. In addition, since the relevant information is the value of the saturation value for each measurement, the program locates the data in a separated array, with the exact time when the measurement was registered ("time stamping").

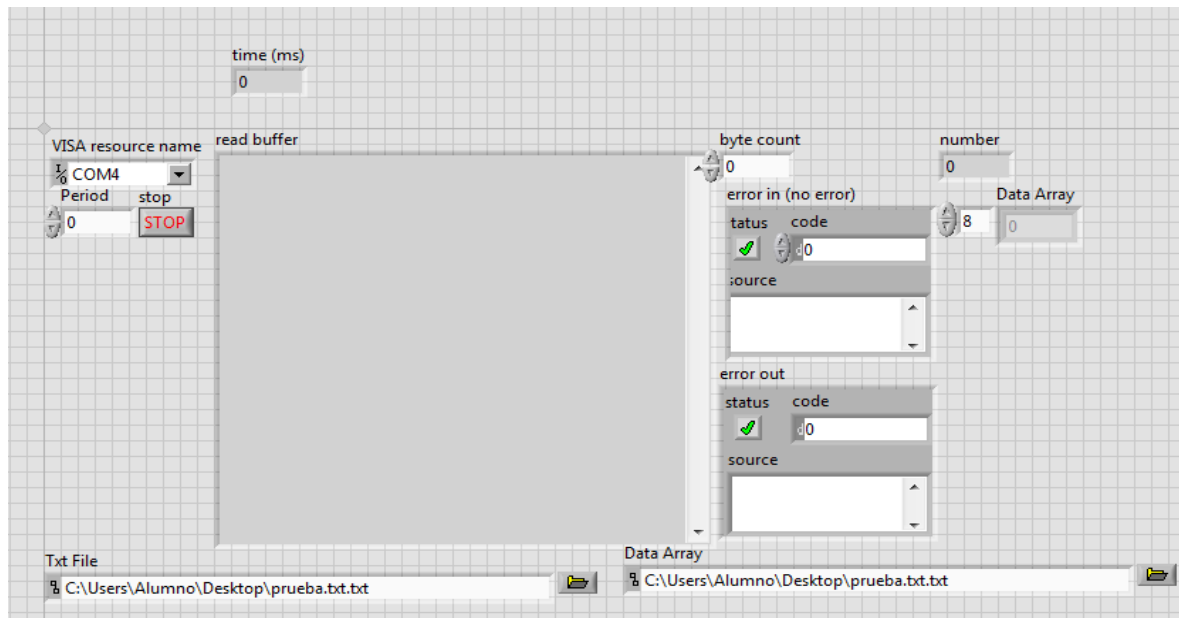


Figure 17. Program interface

The general block diagram of the program is shown in the (Figure 18). The serial port is chosen by VISA command. Once the program recognizes the device connected to the port, the information sent by the device is available for being read and registered. The program reads the information each time the loop (represented by the gray big square) is implemented. The time spent between two consecutive measurements depends on the frequency of the loop. This frequency should be adjusted in order to fulfill with the protocol which the device uses to send the information (in this case, its period is one line per second). Within the loop, part of the information is splitted for recording the saturation event, which is accompanied by the symbol %. The clock represents the *Timestamp*, in milliseconds, of the microcontroller of the computer, and its value is written down every time the loop starts. The information is either written inside and outside the loop in different ways in order to avoid loss of information.



existed between the output of the gas mixer and the animal, and it caused an important delay between the launch of the order execution and the actual moment when the new gas mixture reached the animal. The gas mixer device and the animal were relatively far, because no electronic machinery might enter inside the area delimited by the 5 Gauss field line around the scanner, for security reasons. The dead volume was measured by using syringes of different capacities filled with water and emptied inside the circuit.

Later, after analyzing the information obtained from previous studies, we should decide how many pulseoximeters were going to be utilized and which was actually optimum for our purposes. Moreover, it was important to delimitate when usual oxygen levels must be restored, with the goal of analyzing easily the downward slope of the saturation without compromising animal's safety

Finally, when the required parameters are already settled, image acquisition were performed alternating 100% nitrogen mixture ( nitrogen stage) and 100% oxygen mixture ( oxygen stages), recording in parallel the saturation values using the pulseoximeter device. In addition, obtained images were processed in order to localize the change on the mean intensity in different regions of interest along the whole image sequences.

For all the experiments mentioned above, the mixer set up must be prepared and the corresponding tubes should be connected to the wall gas outlets as shown in (Figure 19). In order to generate a proper flow stream, inline pressure regulators controlled the gas pressure, which was fixed at 1 bar. Moreover, the remote mode of the mixer was established for the purpose of being able to remotely controlling it from the MRI computer.



Figure 19. Gas mixture set up

When all devices were set up, the rat was brought by the technicians to the resonance scanner room to carry out the experiment. The output of the mixer was connected to the inlet of the anesthesia vaporizer, which in turn was connected to a methacrylate box where the animal was anesthetized in the first instance. The chemical used to induce anesthesia was sevoflurane, at 7% during induction process and 3% during maintenance. The composition of the gas generated was 79% N<sub>2</sub> and 21% O<sub>2</sub>, with a flow of 1 liter per minute. After the first experiment, the animal remained at rest with a gas mixture of 100% oxygen. When the animal showed signs of being fully anesthetized, it was moved to the scanner bed, where it remained while the experiment was carried out, and the flow was deviated by a stopcocks system (Figure 21) to the post-vaporizer stage whose tube transits across the roof of the MRI machinery room towards the animal bed.

The animal model chosen for performing the experiments was Wistar rat, three months age, male gender and 300-350g weight. The animal was located onto the table at the entry of the gantry, anesthetized, and its body temperature was preserved by a thermal blanket, warmed by a water circulation system, placed beneath the animal. Once there, technicians recommended reducing the flow generated by the mixer to 400 ml / min.

All procedures and animal handling were performed in accordance with the European directives and national regulations, and under the approval of the Ethics of Animal Experimentation board of the Hospital General Universitario Gregorio Marañón.

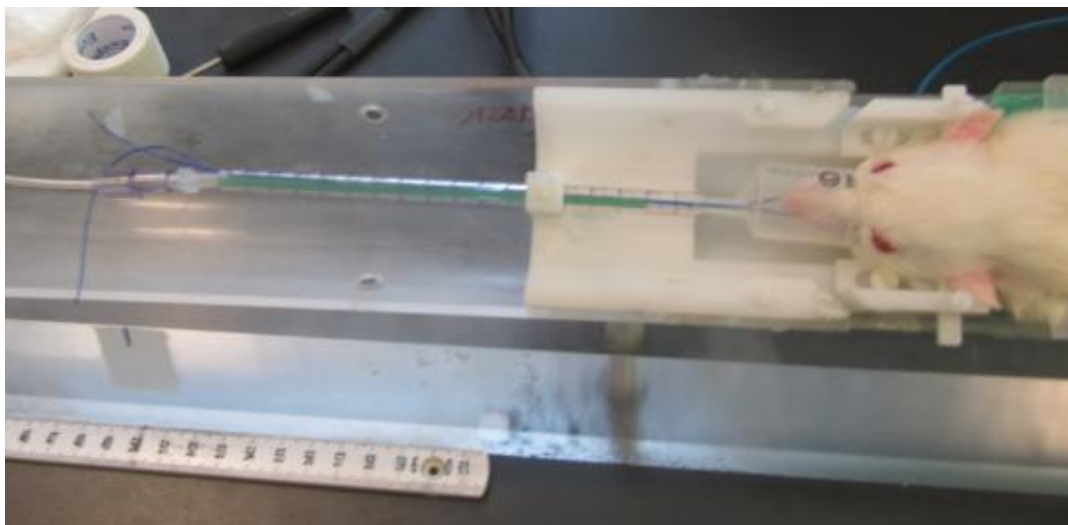


Figure 20. Animal setting



Figure 21. Vaporizer, induction methacrylate box and stopcocks system

Supplementary, in order to control the experiment of image acquisition, an output signal from the scanner is recorded along with the other physiological signals provided by the S.A. control module. The purpose of this procedure was to register the actual beginning of the acquisition process. This output signal followed the TTL standard, and the computer registered its value at any moment. A red LED was placed in line in order to visually assess that its state changed from high (switched on) to low (switched off) whenever the user decided to launch the acquisition.

During the experiment, the diode turned off during one second when image acquisition started, and it remained shining until the pre-established time expired, when it turned off again, and we changed the gas stage to 100% oxygen.

### 3.2.2 Pulseoximeters synchronization

The first problem that arises was that the Masimo pulseoximeter sensor was too large for the rat, and thus achieved a loose fitting when attached to the rat leg. This fact prevented us from assessing whether the measurement obtained was good or bad. We attempted to place the sensor elsewhere, as over the tail. However, no proper measurements were obtained from this location. Therefore, an object (gauze) was inserted to fill the remaining gap, allowing the leg to be attached to the sensor, but the effect of this material on the measure was unknown. In parallel, the animal-devoted pulseoximeter was attached to the other leg. This sensor actually worked, but its measurements were far from being stable (they fluctuate between 60 and 80%), a problem that also appeared with the other device (83-84%). The mixture in this case was composed by 79% nitrogen and 21% oxygen.

However, when a relatively stable measurement was achieved, we proceeded to perform the experiment to see how fast saturation can fall from a fixed value. For this purpose, a new mixture was formed with the same flow but with ratio 100% nitrogen. When saturation began to fall dramatically, the  $FiO_2$  was returned to the initial value to recover the animal, but this time the ratio was 100% oxygen ( $FiO_2=100\%$ ). For synchronization, Masimo's program started readout process when nitrogen stage began, and in the case of the other device this beginning was recorded as an event. Therefore, both curves could be plotted in the same graph with a common time axis.

Finally, it was figured out that by introducing 100% oxygen mixture (instead of 79% nitrogen 21% oxygen), saturation rate reaches 100% in both sensors; therefore, the team proceeded to repeat the above experiment by initially applying 100% nitrogen mixture, and changing to 100% oxygen mixture when the animal's saturation value decreases below 80%.

### 3.2.3 Dead volume

The required measurements were obtained following two stages. Firstly, we measured the tubing volume between the gas mixer and the place where the anesthetic vaporizer was located, since the gas mixer was the actual output of the mixture stream when the order was executed. The mixer and the vaporizer were connected by a flexible tube (as previously shown), whose volume was measured out by means of a 60 ml syringe filled with water. Some pressure was slowly applied to empty the water of the syringe into the flexible tube in order to achieve better accuracy. Some trials were discarded due to air accumulation and bubbles formation in the tube. However, in order to ensure, and even improve, the accuracy and reliability of the measurement, 20 ml and 10 ml capacity syringes were also used.

The second stage included the tubing path from the vaporizer previously mentioned until the final target, where the animal is located during the experiments, that is, the bed located at the entry of the MRI scanner (post-vaporizer stage). Since apparently it was a larger volume compared with the previous stage (since the tube was attached to the ceiling of the room), the strategy followed was to utilize the 60 ml syringe as many times as required so that obtain a first quantitative result, and afterwards using syringes with smaller capacities (20 and 10 ml) to increase precision.

### 3.2.4 Pulseoximeter curves

Although the measurements are slightly different between the two devices, it was unproductive to use both pulseoximeters. The chosen device to be used in the following experiment was the S.A. Instruments one, since it has a special clamp for animals ensuring proper attachment, data recorded were clearly more consistent, and besides it was compatible with magnetic resonance, which avoided any kind of distortion produced by possible electromagnetic interferences induced the pulseoximeter connections.

Bearing in mind the parameters chosen for pulseoximeter synchronization, it was important to study the behavior of the saturation curve depending on the time the 100% nitrogen mixture remained. To that purpose, a respiration sensor was used in order to control the respiratory frequency of the animal. Actually, since pulseoximeter devices in general have a certain delay due to required processing time, breathing rhythm is an important factor to take into account since when oxygen levels decrease, the



respiratory frequency quickly increases, a process known as tachypnea. Presumably, when tachypnea is evident, the recorded values of saturation have might decreased.

During the experiment, the diode turned off during one second when image acquisition started, and it remained shining until the pre-established time expired, which depended on the nitrogen stage duration. Afterwards, the diode turned off again, and we changed the gas mixture to 100% oxygen. Those changes of the diode state were registered in the form of events in the same document as the saturation values, ensuring a common time reference for both the monitoring signals and the MRI signal derived from the images. The measurements were carried out three times for different nitrogen stage durations.

### 3.2.5 Image acquisition

The pulseoximeter clamp was attached to the animal's leg and the animal was prepared in the same way as explained in the synchronization experiment (Figure 22). To acquire the BOLD signal from the brain, a surface coil was placed over the head trying to fix it as tightly as possible in order to avoid any kind of motion which could disturb the posterior study of the information.

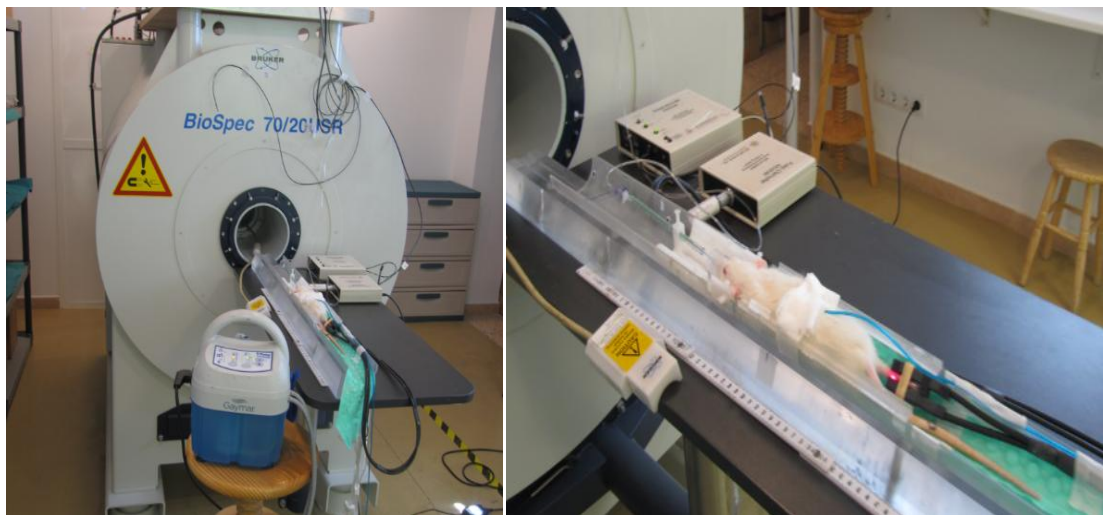


Figure 22. Animal set up

A fast acquisition is extremely important for the purpose of the experiments. Since the changes in saturation values during the falling are very abrupt, the acquisition time of each image must fulfill with the requirements (especially TR and TE) in order to be capable of recording the subsequent changes in MR signal. For that purpose, two different kinds of pulse sequences were used: spin echo planar imaging (SE-EPI) and flash Gradient-Echo (GE).

*Echo planar images* (Figure 23) are extremely fast because the phase encoding step is applied only once in order to fill the whole k-space, whilst in the other types of sequences phase encoding is applied as many times as the number of rows the k-space contains. Therefore, every image is formed in a single TR if no averages are performed. The information needed to form the image is codified from the consecutive gradient-induced echoes. This echo train keeps decaying over time and the spatial resolution of the final image decreases, it needs a special type or reconstruction and this kind of sequences are prone to artefacts formation. However, since our purpose does not address fine anatomical details, spatial resolution is not a crucial factor to consider. The parameters of the sequence were the following: spin echo signal, TR=3s, TE=30.1 ms, matrix size 64 x 64 pixels, 3 slices, slice thickness 2 mm, FOV 20x20 mm, 1 averages, 20 repetitions, total scan time of 60 s.

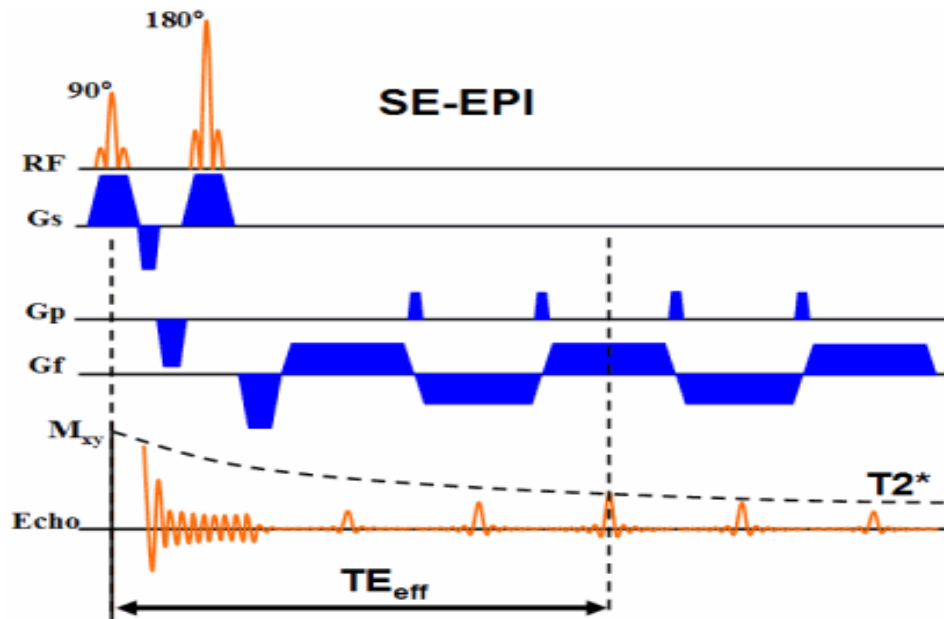


Figure 23 SE- EPI block diagram: Gs represents slice thickness, Gp the phase encoding, Gf the frequency encoding (revisemri.com 2014)

*Gradient echo sequences* (Figure 24) were previously commented in the introduction. The sequence used here is known as FLASH (Fast Low Angle Shot), a gradient echo sequence with low flip angle. However, some techniques and strategies have been carried out in order to speed up the process and shorten acquisition time. One of those strategies relied on conjugate asymmetry. The sequences contain a 1.5 Partial Fourier, which means that the number of rows measured in the k-space (and therefore the number of phase encoding steps) is reduced by a factor of 1.5. The sequence used in our experiment has the following parameters: TR= 5.44 ms, TE= 2.72 ms, matrix size = 128x128 pixels (with 86 lines of direct readout), 1 slice, slice thickness 1,5 mm, FOV 39x 32 mm, 2 averages, 65 repetitions, total scan time of 60.84 seconds.

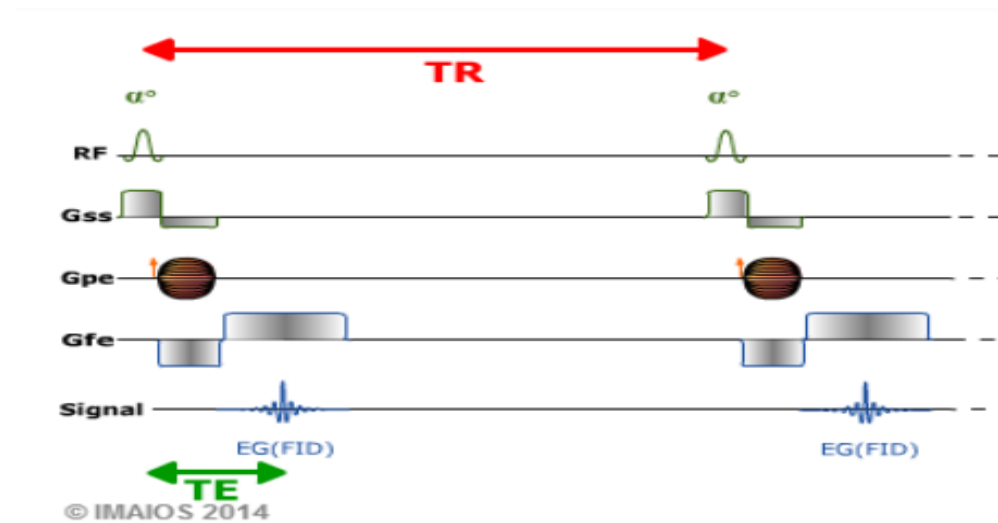


Figure 24. EPI block diagram: Gss represents slice thickness, Gpe the phase encoding, Gfe the frequency encoding

Three sequences were selected for further processing; two EPIs (EPI 15 and EPI 16) and one FLASH (flash 17).

### 3.2.6 Image processing

In order to quantify the behavior of the signal over time, the three slices of each EPI sequences were independently analyzed by means of the free and public software ImageJ (<http://imagej.nih.gov/ij/>). Different anatomical features were selected as regions of interest (ROI) in order to study how mean intensity changed in certain zones of the images. The values of the mean intensity of each ROI were

computed by using ImageJ and Matlab, joined with the saturation curve obtained from the values of the pulseoximeter during each respective acquisition process.

## **4 Results**

### **4.1 Pulseoximeters synchronization**

Data measured by the two devices were collected and recorded by their respective software programs. The information was afterwards processed and plotted using Matlab software, as illustrated in (Figure 25). We observed a significant delay between the responses of both pulseoximeters, since values recorded with the S.A. Instruments' device showed a fall earlier than the other one. Moreover, the fall slope was higher in S.A Instruments device, it decreases almost 2.4 % per second in comparison with the 0.7% of the Masimo. Besides, the amplitude reached by the Instruments' one is larger. Our results suggest the existence of a strong signal filtering in the Masimo device which finally made it advisable not to use it for the imaging session.

We also observed a long delay between the start of the 100% nitrogen mixture and the start of the S.A. decay, which suggested the existence of an important dead volume effect in the tubing that needed to be measured.

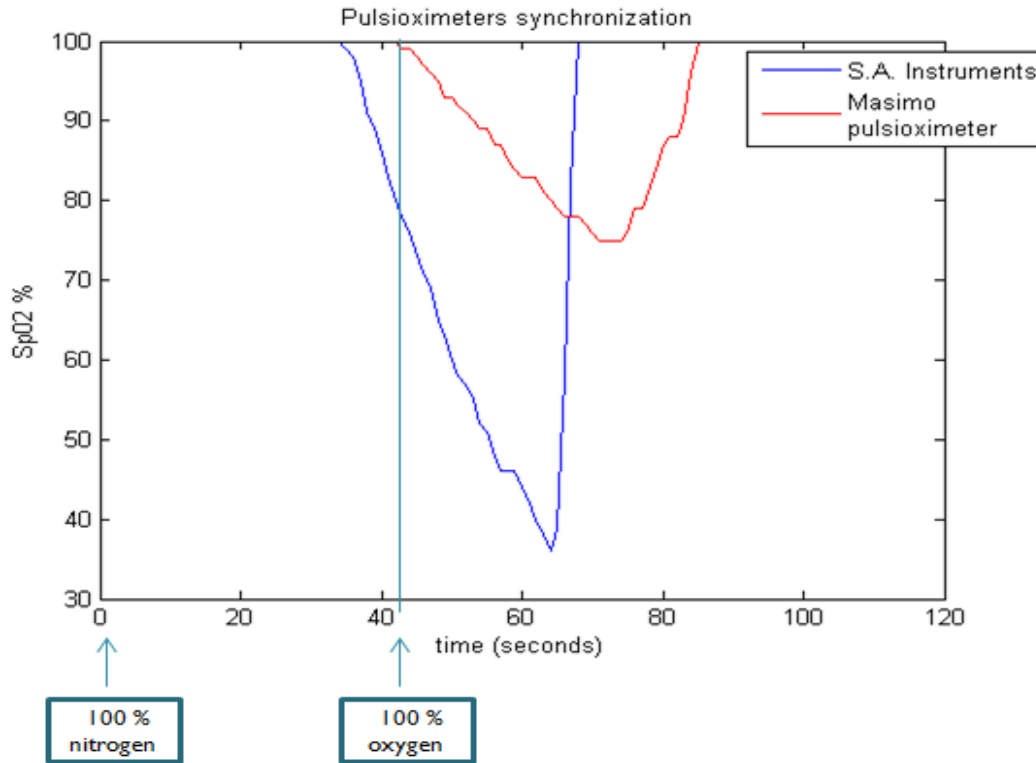


Figure 25

## 4.2 Dead volume

Large syringe volume was 60 ml, and small syringes volumes were 20 and 10 ml. For the pre-vaporizer stage, the final result yielded 29,2 ml, vs. a theoretical estimation of 30 ml at the beginning. For the second stage, two measurements were carried out following the procedure mentioned before; 72,5 and 72,7 , both in milliliters. For the final volume for post-vaporizer stage we took the mean of both measurements, that is, 72,6 ml. Therefore, the final dead volume of the whole system was approximately 101,8 ml.

The errors introduced by the syringes measurements should be taken into account, since it would introduce some delay in the expected time spent by the mixture to reach the animal. The error due to the syringes is half a milliliter. Since the total flow for pulseoximeter synchronization experiments was 400 ml/ min, the temporal estimated error is roughly 150 milliseconds. The error may be tolerated as

long as it is small enough compared with the error introduced by ourselves during the activation of the several mechanisms which form part of the experiments (around 1 second).

Therefore, assuming 101,8 ml as total dead volume from the gas mixer to the animal, and 400 ml/min flow, the delay in our signal, either in pulseoximeter and images, introduced by the dead volume of the circuit was estimated in 15,3 seconds, with the error previously reported. This number matches did not match exactly with the delay measured (roughly 20 seconds), since saturation did not drop instantaneously when 100% nitrogen mixture arrived to the animal. This may be mainly by the autoregulation mechanisms, that is, delay introduced by the animal itself.

### 4.3 Pulseoximeter curve profile

The data collected were plotted in three different graphics, depending on the duration of nitrogen stages. The vertical line parallel to the Y-axes represents when the mixtures change to 100% oxygen, instead of the initial 100% nitrogen. Figure 26 represents the change of mixture at 18 seconds; Figure 27 represents the change of mixture at 21 second; Figure 28 represents the change of mixture at 24 seconds. Breathing rate is also plotted to visualize its change during hypoxia.

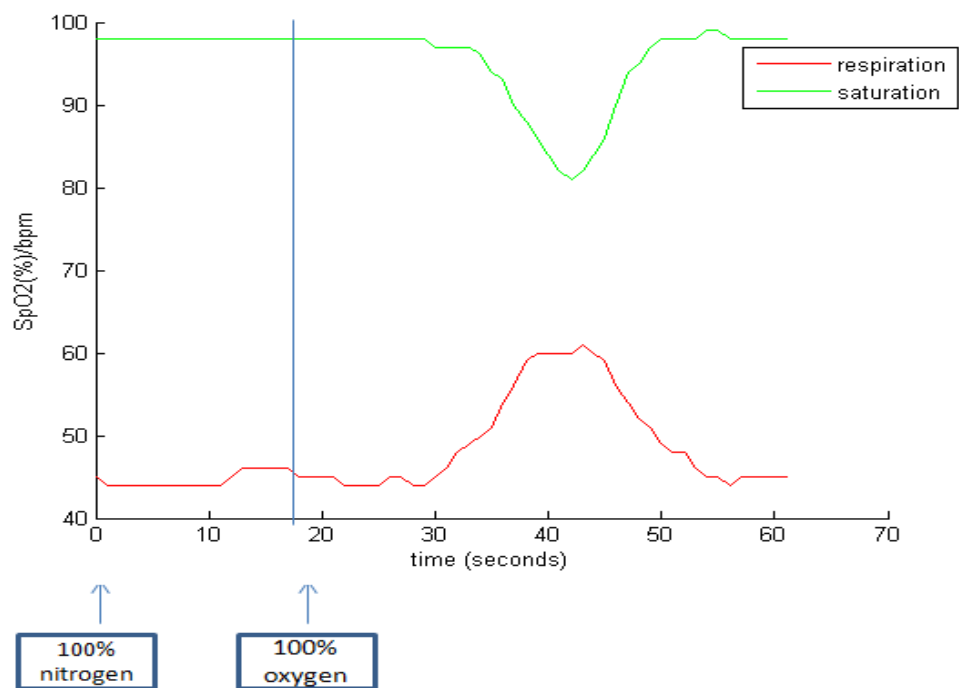


Figure 26

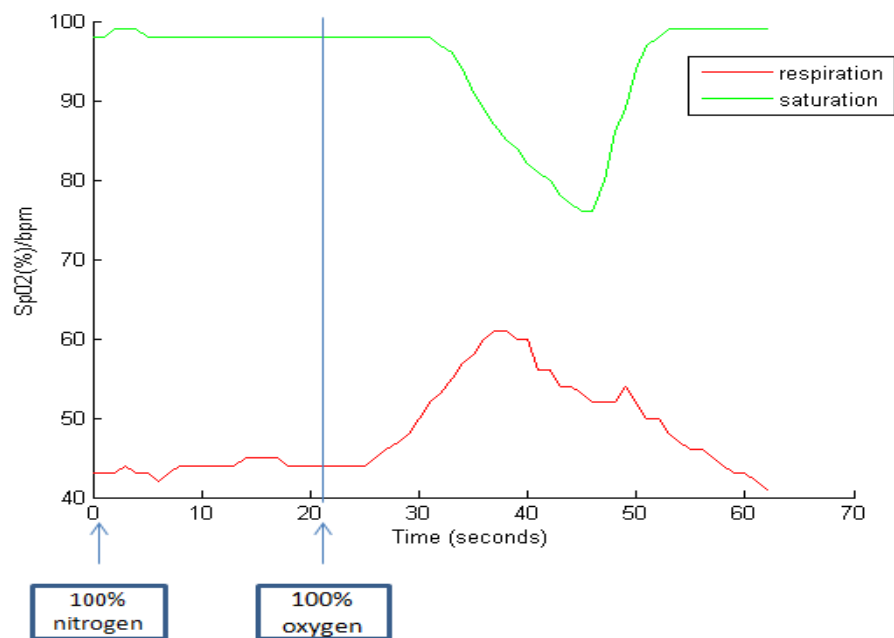


Figure 27

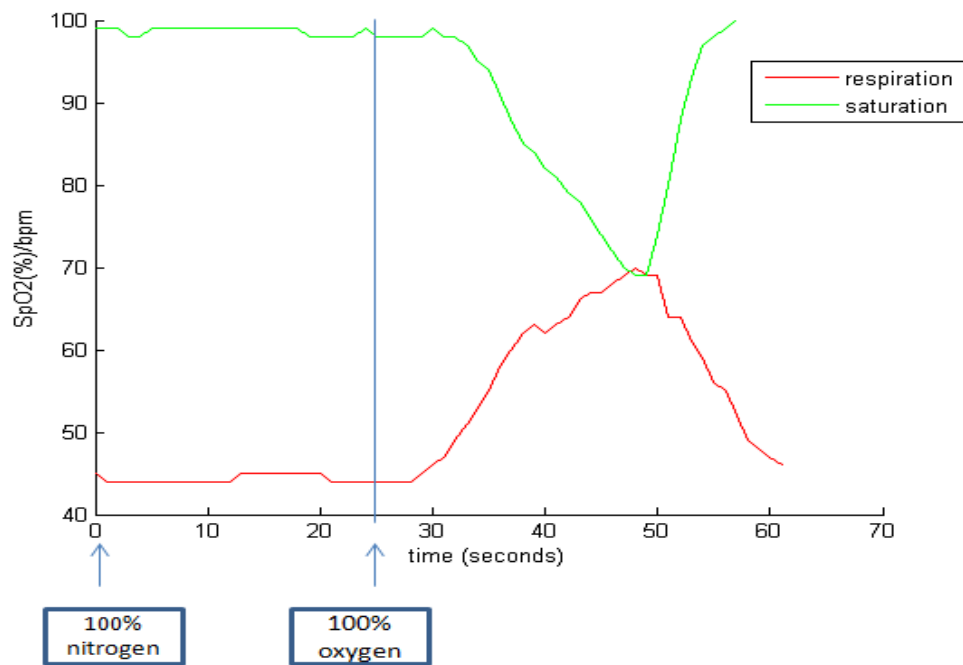


Figure 28

#### 4.4 Image acquisition

This section presents the images acquired, two EPI sequences with three slices each sequence, and 20 frames per slice. On the other hand, one Flash GE sequence with only one slice and 65 frames.

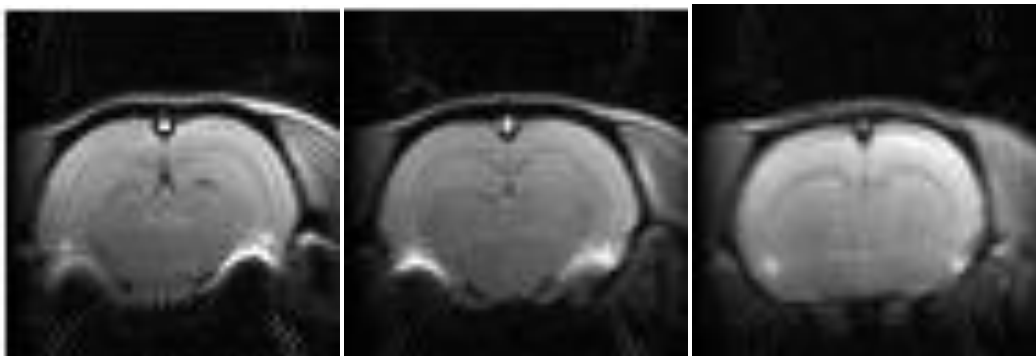


Figure 29. EPI 15 sequence. Same frame (10/20) for the different slices. First slice on the left, second at the center, third on the right



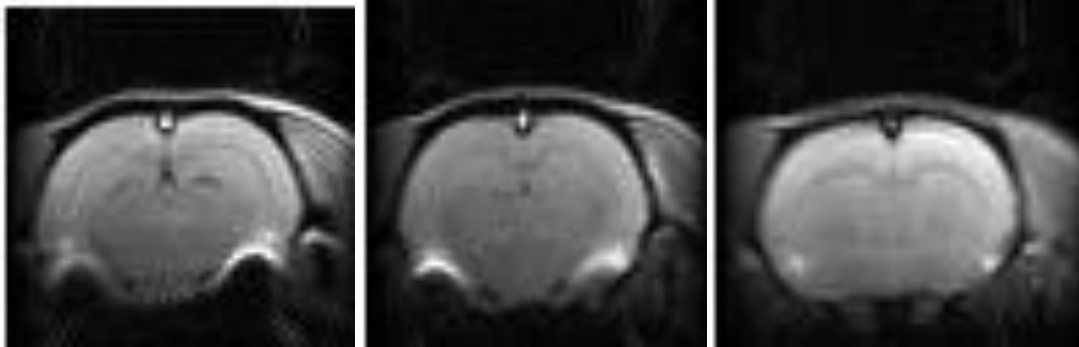


Figure 30. . EPI 16 sequence. Same frame (10/20) for the different slices. First slice on the left, second at the center, third on the right

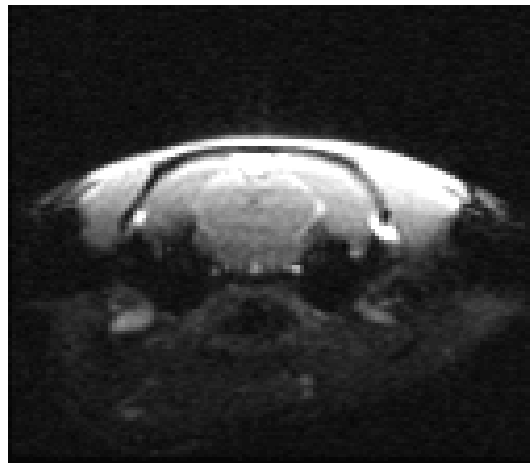


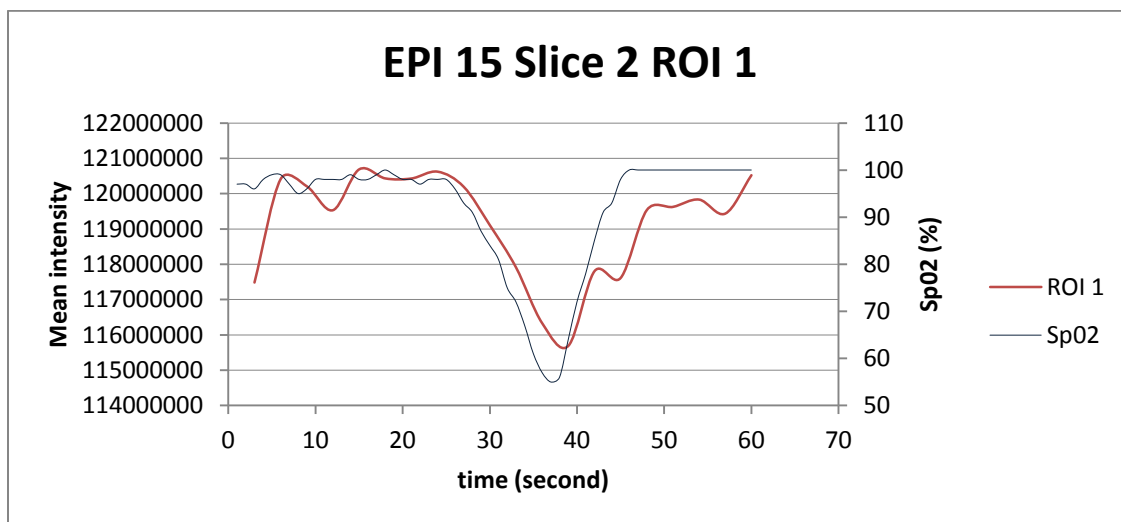
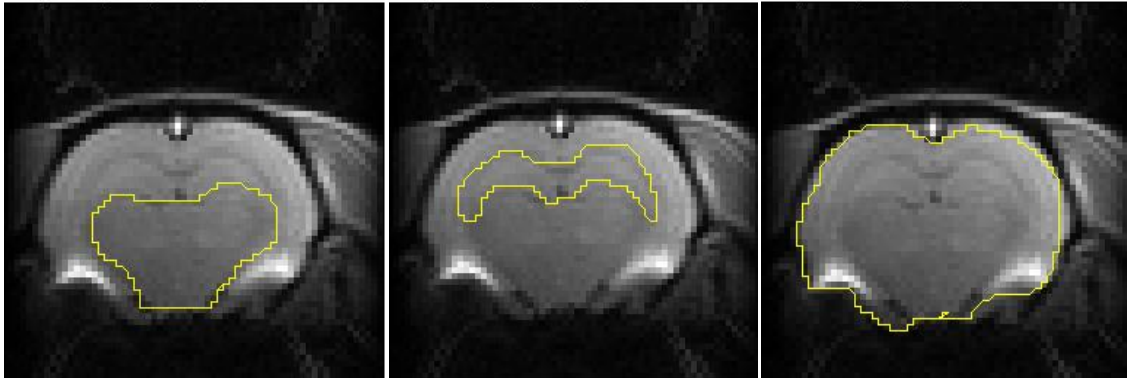
Figure 31. Flash GE sequence image

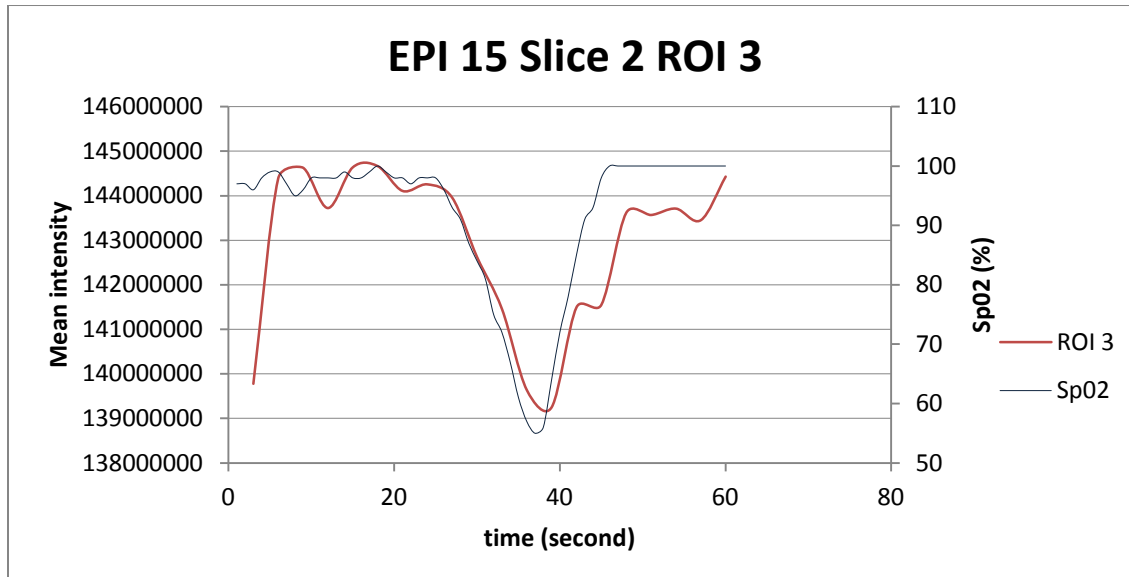
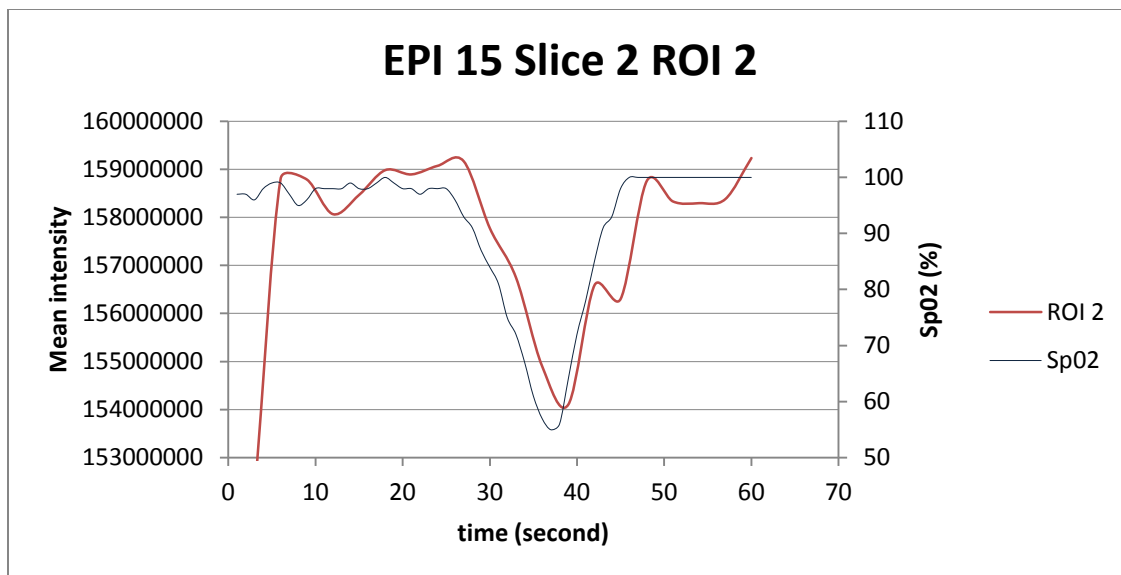
## 4.5 Image processing

The regions of interest selected and the evolution of their intensities over the temporal repetitions are shown below, together with their corresponding saturation curves. In all the cases presented below, ROI 1 2 and 3 are ordered from left to right. The mean intensity in the SE-EPI sequences decreases when the oxygen levels of blood decrease, as shown in the graphs below.

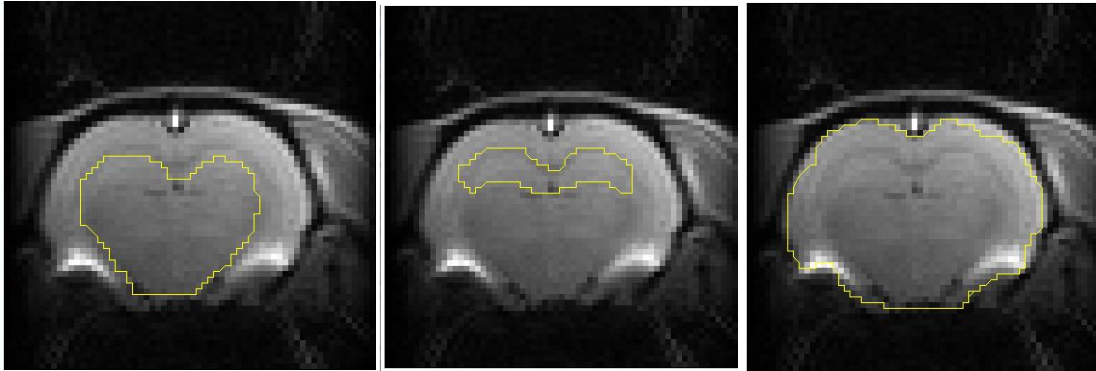
In the second slice of both EPIs, this drop is more evident and neat; this is the reason why the three graphs shown below belong to this slice.

*EPI 15 slice 2*

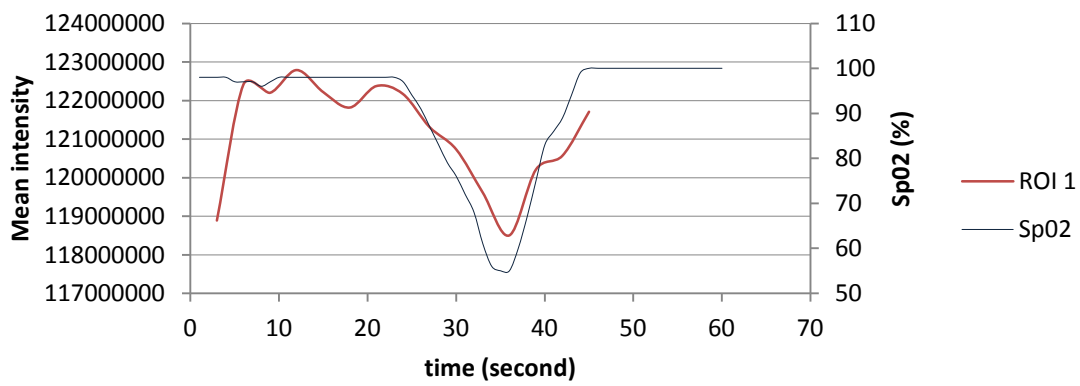




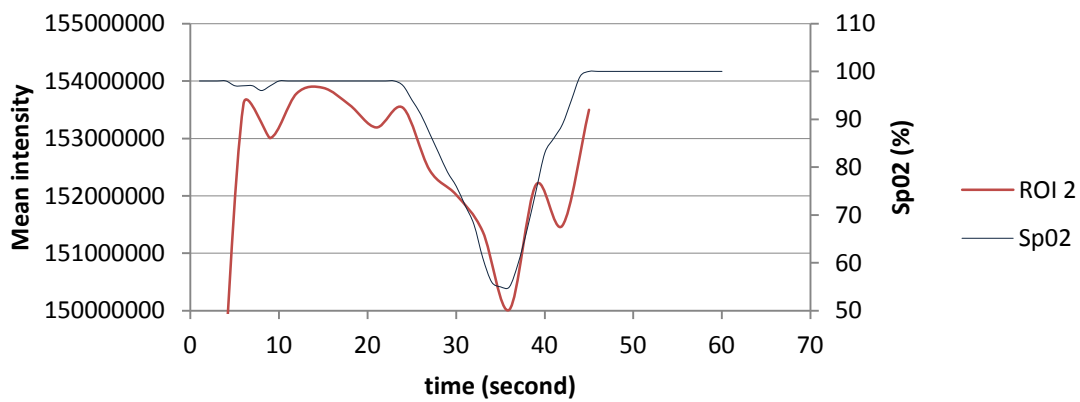
EPI 16 second slice

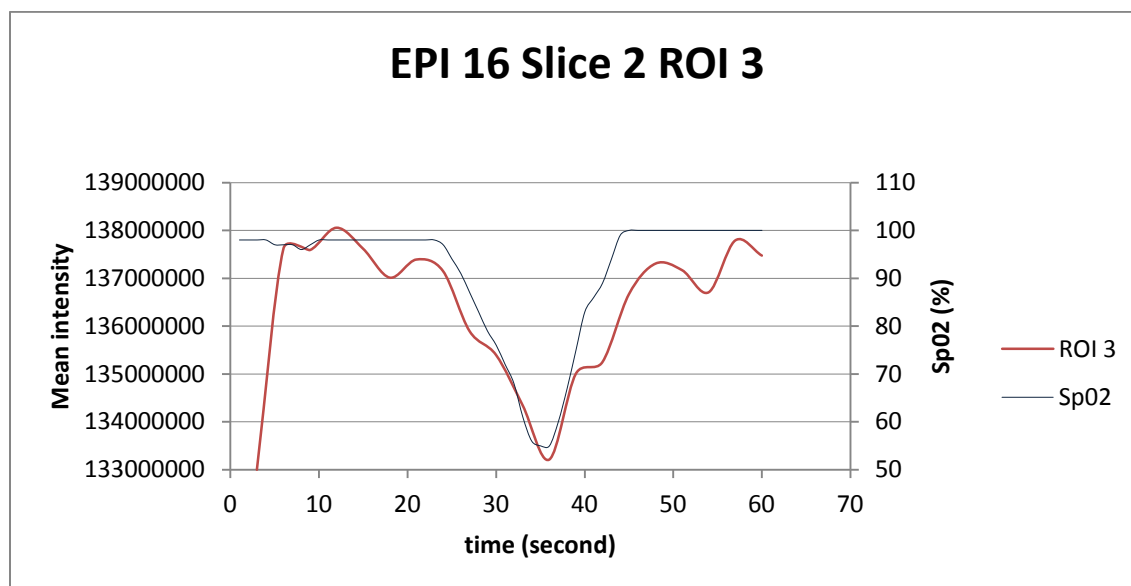


**EPI 16 Slice 2 ROI 1**

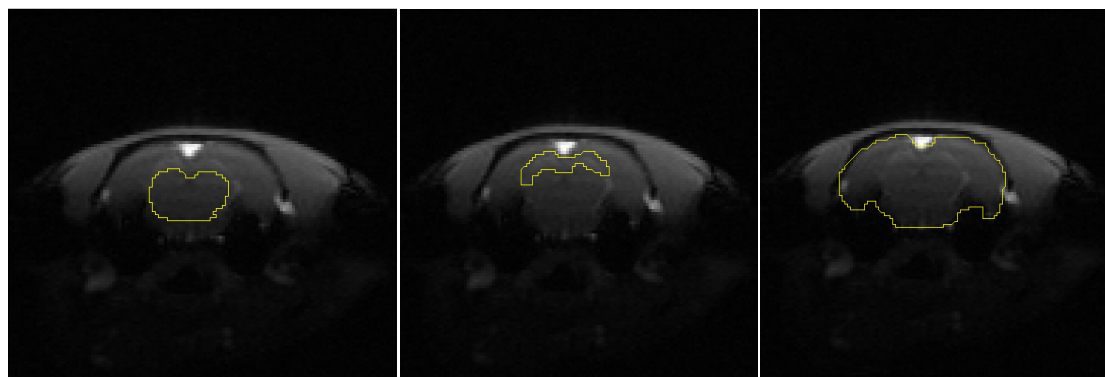


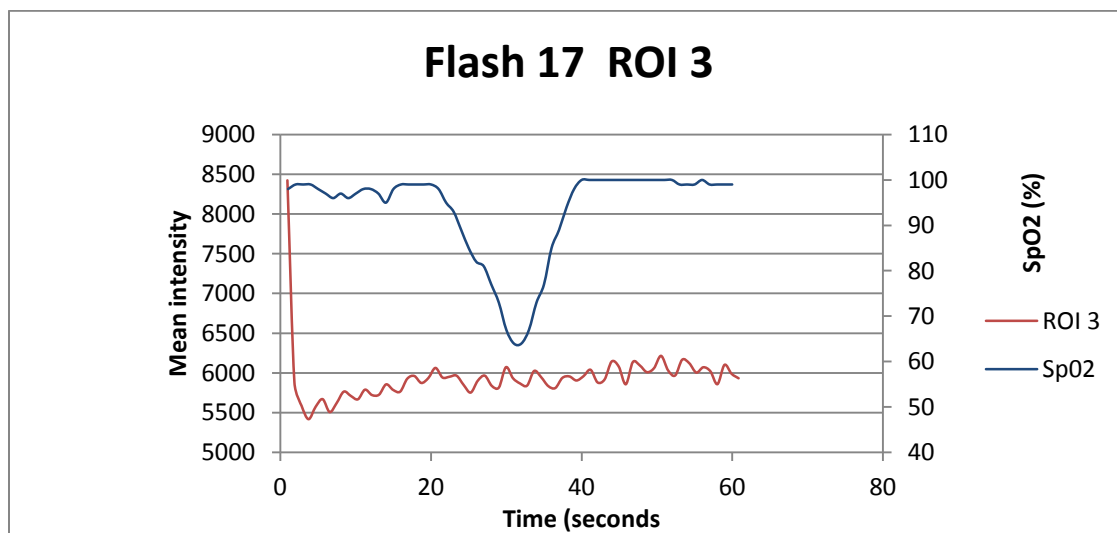
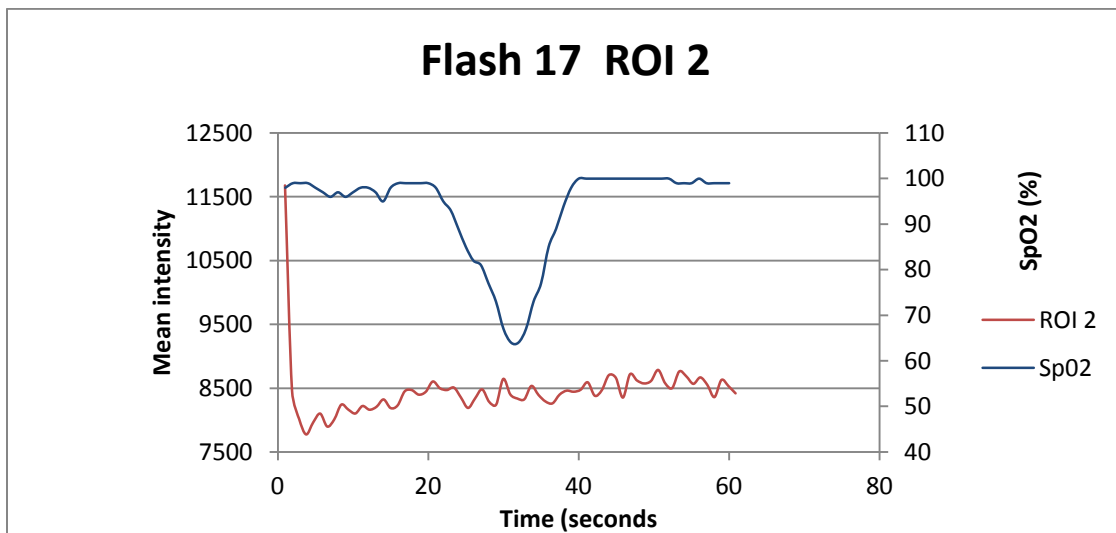
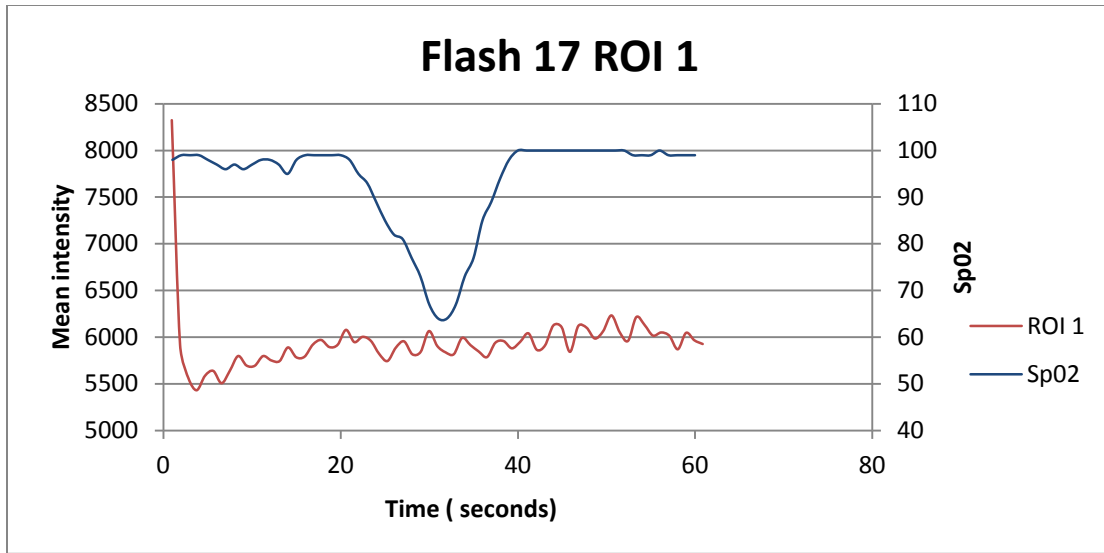
**EPI 16 Slice 2 ROI 2**





Flash 17





## 5 Discussion and conclusions

### 5.1 General discussion

The results show unequivocally that under certain conditions, when the levels of oxygen in blood are reduced considerably, the mean intensity of the reconstructed images drops, in a similar way (delayed) as the saturation curve recorded by the pulseoximeter device. Thus, when concentrations of deoxyhemoglobin raise, the change in the recorded signal leads to a darkening of the image. Besides, when normal oxygen levels are established again, mean intensity in the images recovers its initial value. Therefore, this is a proof of concept that own blood could be utilized as endogenous contrast to determine the degree of perfusion in a certain brain structure.

However, some details must be taken into account when the final results of the project are analyzed, and some of them deserve a deeper and careful study. One of the parameters which could somehow disturb our experiment is how fast the pulseoximeter devices process and display the information. Generally, these kinds of devices compute several measurements and average before the final result is displayed. Moreover, in order to avoid the effect of non-pulsatile tissue structures, they apply several filter steps, which seem to slow down the processing. In addition, rapidness of the system varies from one device to another (as shown in the results), so some degree of timing uncertainty due to the instrumentation can be expected. Besides, not only the devices delay the process; also the animal could introduce some disturbance regarding the time point at which the saturation starts to decrease. This is due to the auto regulation mechanisms which tightly control the amount of oxygen and nutrients delivered to the tissue depending on several conditions, which the body is able to detect and counteract. Therefore, saturation values take some time to decrease from the moment when nitrogen gas stage is inhaled by the animal, and this delay may also vary depending on the animal characteristics (age, weight, gender...). This is the reason why a respiration sensor has been incorporated to the system, in order to determine when the body actually starts to be aware of that drop in the inhaled oxygen. Obviously, tachypnea occurs before the saturation curve from the pulseoximeter readings start to decrease, thus suggesting that the body reaction is faster than the pulseoximeter.

As far as the rest of the machinery is concerned, synchronization among them is important due to the number of devices needed to carry out the whole process. In our experiments, the most difficult

synchronization problem was between the scanner and the mixer, because both were launched by hand. Besides, the scanner also spends some time making internal adjustments before the data starts to be digitized and recorded, so the image acquisition process does not start immediately. In order to accurately determine the different delays until the saturation drops, the gas mixer order should be launched at the same time the acquisition starts.

High deoxyhemoglobin concentrations disturbs the previous magnetic conditions of the sample, provoking a faster dephase of the spins and subsequently a faster decrease of the signal, leading to a drop of the mean intensity in the image. However, the chosen sequences must contain certain parameters in order to make this effect noticeable. BOLD effect is more evident in T2-weighted images. T2 weighted images require a long TR and a long TE. In the SE- EPI sequences used, TR and TE are long enough and TE of the sequence is very similar to T2 parameter in the brain. Therefore, the signal must decrease when the levels on inhaled oxygen are reduced.

In the case of gradient echo sequences, almost no change is noticeable. This could be due to its low value of TR and TE, leading to a more T1 weighted for the brain tissue in which BOLD signal cannot be detected. Therefore, since TE is not similar to the T2 value of the brain (because it had been adjusted and optimized for dynamic contrast studies in abdominal tumors), the parameters should be re-adjusted in order to perceive the required signal in the brain.

In conclusion, the actual response of the saturation curve through a pulseoximeter during changes in the percentage of inhaled oxygen has been characterized and secondly, recording of the changes in MRI signal in the images due to the application of those changes through the use of dynamic sequences has been accomplished. Nevertheless, the results are difficult to extrapolate to the clinical environment, since the strength of the magnetic field used for the experiment is very high (7T) compared to the usual values used with humans for clinics (1.5-3 T). At those lower field strength levels, the signal from large vessels could disrupt the effect of the capillaries, which is in fact the important signal analyzing perfusion in the brain. However, it opens up a new range of possibilities regarding research and preclinical investigation.



## 5.2 Future experiments and improvements

There are several improvements which could be implemented in the future in order to optimize the experiments. The first issue to improve would be the full automation of the process, including the synchronization between the gas mixer and the MRI scanner. *Paravision* software of the BRUKER scanner allows introducing lines of C language into its routines in order to work together with other devices. This fact would avoid accumulation of timing errors due to manual orders execution, since it would automatically change the gas mixer during image acquisition accordingly with the selected parameters. However, C language code should be located in a very specific place in very specific manner, and some tests are required to ensure feasibility.

Other improvement is the re-adjust of the parameters of those sequences which have not achieved conclusive results, by modifying and calibrating parameters as TE in order to make them coincide with those of the brain.

Finally, the results obtained in the project open up the possibility of modeling mathematically the behavior of the perfusion in several brain compartments or regions, using kinetic modeling and differential equations, which would lead to a real quantification of the tissue perfusion.

## 6 References

1. Suetens, P., *Fundamentals of medical imaging*. . 2002.: Cambridge University Press.
2. Gibby, A., *Basic principles of magnetic resonance imaging*. Neurosurgery clinics of North America, January 2005. **16**(1): p. 1-64.
3. Callaghan, P., *Principles of Nuclear Magnetic Resonance Microscopy*. Oxford University Press, 1994.
4. Brown, M., *MRI: Basic principles and applications*. . 2003: Willey-Liss Publications.
5. Buxton, R., *Introduction to functional magnetic resonance imaging: Principles and techniques*. 2002: Cambridge University Press.
6. *MRI step-by-step, interactive course on magnetic resonance imaging*  
Available from: <http://www.imaio.com/en/e-Courses/e-MRI>.
7. McRobbie, *MRI from picture to proton*. 2003. 359-60.
8. Carpenter, T.A., *MRI - from basic knowledge to advanced strategies: hardware*. European radiology, 1999. **9**(6): p. 1015-9.
9. Shellock, *MRI safety, bioeffects and patient management*. Biomedical Research Publishing Group, Los Angeles, CA, 2001.
10. Dale, P., *Neuroscience*. Sinauer Associates, 2008: p. 834-5.
11. Walters, F., *Intracranial Pressure and Cerebral Blood Flow*. Physiology, 1998(8).
12. Ogawa, S., et al., *Brain magnetic resonance imaging with contrast dependent on blood oxygenation*. Proc Natl Acad Sci USA, 1990. **87**(24): p. 9868-72.
13. Thulbom, K.R., *Oxygenation dependence of the transverse relaxation time of water protons in whole blood at high field*. Biochim Biophys Acta, Feb 1982. **714**(2): p. 265-70.
14. Kwong, K.K., *Dynamic magnetic resonance imaging of human brain activity during primary sensory stimulation*. Proc. Natl. Acad. Sci. USA, 1992. **89**: p. 5675-9.
15. Framh, J., *Dynamic MR imaging of human brain oxygenation during rest and photic stimulation*. J. Magn. Reson. Imag, 1992. **2**: p. 501-5.
16. Ogawa, S., *Intrinsic signal changes accompanying sensory stimulation: Functional brain mapping with magnetic resonance imaging*. . Proc. Natl. Acad. Sci. USA, 1992. **89**: p. 5951-5.

17. Bendettini, P.A., *Time course EPI of human brain function during task activation* Magn. Reson. Med, 1992. **25**: p. 390-7.
18. Uğurbil, K., *TWO DECADES OF FUNCTIONAL IMAGING: FROM NUCLEAR SPINS TO CORTICAL COLUMNS*.
19. Uludağ, K. , *An integrative model for neuronal activity-induced signal changes for gradient and spin echo functional imaging*. NeuroImage 2009. **48**: p. 150-165.
20. Duschek, S., *Reduced brain perfusion and cognitive performance due to constitutional hypotension*. Clinical Autonomic Research, 2007. **17**(2): p. 69-76.
21. van Beek, A.C., ; Rikkert, M.G.; Jansen, R.W., *Cerebral autoregulation: An overview of current concepts and methodology with special focus on the elderly*. Journal of Cerebral Blood Flow & Metabolism June 2008. **28**(6): p. 1071-85.
22. Geraldès, C., *Classification and basic properties of contrast agents for magnetic resonance imaging*. Contrast Media & Molecular Imaging, 2009. **4**(1): p. 1-23.

# Supplementary material

## C-language gas mixer program

### -Legend

Mixgas [0=OFF, 1=ON] [Channel no. from 1 to 4] [Gas 1] [Percentage Gas 1] [Gas 2] [Percentage Gas 2]  
[Gas 3] [Percentage Gas 3] [Total Flow ml/min]

Gas numbers: 1=air,2=N2,3=O2,4=CO2,5=He,6=Ar,7=CO,8=Ne,9=NO,10=N2O,11=SF6,12=Xe,13=CH4

### -Code

```
*****
```

```
* Copyright (C) 2009 by lacayo *
* lacayo@localhost.localdomain *
* This program is free software; you can redistribute it and/or modify *
it under the terms of the GNU General Public License as published by *
* the Free Software Foundation; either version 2 of the License, or *
* (at your option) any later version. *
* This program is distributed in the hope that it will be useful, *
* but WITHOUT ANY WARRANTY; without even the implied warranty of *
* MERCHANTABILITY or FITNESS FOR A PARTICULAR PURPOSE. See the *
* GNU General Public License for more details. *
* You should have received a copy of the GNU General Public License *
* along with this program; if not, write to the *
* Free Software Foundation, Inc., *
* 59 Temple Place - Suite 330, Boston, MA 02111-1307, USA. *
```

```
*****/
```

```
#ifdef HAVE_CONFIG_H
#include <config.h>
#endif
```

```

#include <stdio.h>

#include <stdlib.h>

#include <math.h>

#include <malloc.h>

#include <unistd.h>

#include "./rs232.h"

FILE *loggg;

int main( int argc, char *argv[] )

{

    int numclosed;

    int error=0;

    int i,err,num,a1,a2,a3,a4;

    float ar1,ar2,ar3,ar4,ar5,ar6,ar7,ar8,ar9,ar10,ar11,ar12;

    unsigned char p11,p12,p21,p22,p31,p32,t1,t2;

    char *aux;

    //*****LOG*****

    if( (loggg = fopen( "./log.txt","w")) ==NULL )

        fprintf(loggg,"The file 'log.txt' was not opened\n" );

    else

        fprintf(loggg, "The file 'log.txt' was opened\n" );

    //*****OPENPORT*****

    if(OpenComport(0,19200)==1) fprintf(loggg,"COM1 NOT OPENED\n");

        else fprintf(loggg,"COM1 OPENED\n");

    // printf("Argc = %d\n",argc);

    if ((argc == 10) || (argc ==2)){ printf("Correct no. of arguments\n\r");}

    else{ printf("Incorrect number of arguments. Syntax is \n\r");

        printf("\n\r");

        printf("Mixgas [0=OFF, 1=ON] [Channel no. from 1 to 4] [Gas 1] [Percentage Gas 1] [Gas 2] [Percentage Gas 2] [Gas 3] [Percentage Gas 3] [Total Flow ml/min]\n\r");
    }
}

```

```

        printf("Remember gas numbers:
1=air,2=N2,3=O2,4=CO2,5=He,6=Ar,7=CO,8=Ne,9=NO,10=N2O,11=SF6,12=Xe,13=CH4\n\r"); return (-1);

        printf("\n\r"); }

if (argc == 10){

        //Parsing args

        ar1=(float)atoi(argv[1]);

        ar2=(float)atoi(argv[2]);

        ar3=(float)atoi(argv[3]);

        ar4=(float)atoi(argv[4]);

        ar5=(float)atoi(argv[5]);

        ar6=(float)atoi(argv[6]);

        ar7=(float)atoi(argv[7]);

        ar8=(float)atoi(argv[8]);

        ar9=(float)atoi(argv[9]);

        //Checking args

if (ar1!=1){

        printf("First argument must be 1 to turn ON. Syntax is \n\r");

        printf("\n\r");

        printf("Mixgas [0=OFF, 1=ON] [Channel no. from 1 to 4] [Gas 1] [Percentage Gas 1] [Gas 2] [Percentage
Gas 2] [Gas 3] [Percentage Gas 3] [Total Flow ml/min]\n\r");

        printf("Remember gas numbers:
1=air,2=N2,3=O2,4=CO2,5=He,6=Ar,7=CO,8=Ne,9=NO,10=N2O,11=SF6,12=Xe,13=CH4\n\r"); return (-1);

        printf("\n\r");

}

if ((ar2<1) || (ar2>4)){

        printf("Second argument must be from 1 to 4, it indicates the mixer channel. Syntax is \n\r");

        printf("\n\r");

        printf("Mixgas [0=OFF, 1=ON] [Channel no. from 1 to 4] [Gas 1] [Percentage Gas 1] [Gas 2] [Percentage
Gas 2] [Gas 3] [Percentage Gas 3] [Total Flow ml/min]\n\r");

        printf("Remember gas numbers:
1=air,2=N2,3=O2,4=CO2,5=He,6=Ar,7=CO,8=Ne,9=NO,10=N2O,11=SF6,12=Xe,13=CH4\n\r"); return (-1);

        printf("\n\r");

```

```

}

if ((ar3<1) || (ar3>13)){

    printf("Gas 1 must be indicated with a number from 1 to 13. Syntax is \n\r");

    printf("\n\r");

    printf("Mixgas [0=OFF, 1=ON] [Channel no. from 1 to 4] [Gas 1] [Percentage Gas 1] [Gas 2] [Percentage Gas 2] [Gas 3] [Percentage Gas 3] [Total Flow ml/min]\n\r");

    printf("Remember gas numbers:
1=air,2=N2,3=O2,4=CO2,5=He,6=Ar,7=CO,8=Ne,9=NO,10=N2O,11=SF6,12=Xe,13=CH4\n\r"); return (-1);

    printf("\n\r");

}

if ((ar5<1) || (ar5>13)){

    printf("Gas 2 must be indicated with a number from 1 to 13. Syntax is \n\r");

    printf("\n\r");

    printf("Mixgas [0=OFF, 1=ON] [Channel no. from 1 to 4] [Gas 1] [Percentage Gas 1] [Gas 2] [Percentage Gas 2] [Gas 3] [Percentage Gas 3] [Total Flow ml/min]\n\r");

    printf("Remember gas numbers:
1=air,2=N2,3=O2,4=CO2,5=He,6=Ar,7=CO,8=Ne,9=NO,10=N2O,11=SF6,12=Xe,13=CH4\n\r"); return (-1);

    printf("\n\r");

}

if ((ar7<1) || (ar7>13)){

printf("Gas 3 must be indicated with a number from 1 to 13. Syntax is \n\r");

printf("\n\r");

printf("Mixgas [0=OFF, 1=ON] [Channel no. from 1 to 4] [Gas 1] [Percentage Gas 1] [Gas 2] [Percentage Gas 2] [Gas 3] [Percentage Gas 3] [Total Flow ml/min]\n\r");

    printf("Remember gas numbers:
1=air,2=N2,3=O2,4=CO2,5=He,6=Ar,7=CO,8=Ne,9=NO,10=N2O,11=SF6,12=Xe,13=CH4\n\r"); return (-1);

    printf("\n\r");

}

```

```

if ((ar4<0)|| (ar4>100)|| (ar6<0)|| (ar6>100) || (ar8<0) || (ar8>100))  {

    printf("Percentages of gases must be from 0 to 100. Syntax is \n\r");

    printf("\n\r");

    printf("Mixgas [0=OFF, 1=ON] [Channel no. from 1 to 4] [Gas 1] [Percentage Gas 1] [Gas 2] [Percentage Gas 2] [Gas 3] [Percentage Gas 3] [Total Flow ml/min]\n\r");

    printf("Remember gas numbers:
1=air,2=N2,3=O2,4=CO2,5=He,6=Ar,7=CO,8=Ne,9=NO,10=N2O,11=SF6,12=Xe,13=CH4\n\r"); return (-1);

    printf("\n\r");

}

if ((ar4+ar6+ar8)!=100)  {

    printf("Percentages of gases must add up 100. Syntax is \n\r");

    printf("\n\r");

    printf("Mixgas [0=OFF, 1=ON] [Channel no. from 1 to 4] [Gas 1] [Percentage Gas 1] [Gas 2] [Percentage Gas 2] [Gas 3] [Percentage Gas 3] [Total Flow ml/min]\n\r");

    printf("Remember gas numbers:
1=air,2=N2,3=O2,4=CO2,5=He,6=Ar,7=CO,8=Ne,9=NO,10=N2O,11=SF6,12=Xe,13=CH4\n\r"); return (-1);

    printf("\n\r");

}

if ((ar9<0)|| (ar9>10101010101010101010000))  {

    printf("Total flow must be from 0 to 3000 (ml/min). Syntax is \n\r");

    printf("\n\r");

    printf("Mixgas [0=OFF, 1=ON] [Channel no. from 1 to 4] [Gas 1] [Percentage Gas 1] [Gas 2] [Percentage Gas 2] [Gas 3] [Percentage Gas 3] [Total Flow ml/min]\n\r");

    printf("Remember gas numbers:
1=air,2=N2,3=O2,4=CO2,5=He,6=Ar,7=CO,8=Ne,9=NO,10=N2O,11=SF6,12=Xe,13=CH4\n\r"); return (-1);

    printf("\n\r");

```



```

    }
    // for (i=1;i<argc;i++){printf("%s\n",argv[i]);}
    // _____ CODE _____

    // Conversions of %

    ar4*=10;

    ar6*=10;

    ar8*=10;

    a1=(int)ar4;

    p12=(unsigned char)a1%256;

    p11=(unsigned char)(int)(a1/256);

    a2=(int)ar6;

    p22=(unsigned char)a2%256;

    p21=(unsigned char)(int)(a2/256);

    a3=(int)ar8;

    p32=(unsigned char)a3%256;

    p31=(unsigned char)(int)(a3/256);

    a4=(int)ar9;

    t2=(unsigned char)a4%256;

    t1=(unsigned char)(int)(a4/256);


    unsigned char buf[12]={(unsigned char)ar2,(unsigned char)ar3,p11,p12,(unsigned char)ar5,p21,p22,(unsigned
char)ar7,p31,p32,t1,t2};

    num=SendBuf(0,buf,sizeof(buf));

    fprintf(loggg,"Number of bytes sent to mixer: %d\n",num);
}

else if (argc==2){ //if we want to turn it OFF, send '9'

    ar1=(float)atoi(argv[1]);

    if(ar1!=0){

```

```

        printf("First and only argument must be 0 to turn OFF. Syntax is \n\r");

        printf("\n\r");

        printf("Mixgas [0=OFF, 1=ON] [Channel no. from 1 to 4] [Gas 1] [Percentage Gas 1] [Gas 2]
[Percentage Gas 2] [Gas 3] [Percentage Gas 3] [Total Flow ml/min]\n\r");

        printf("Remember gas numbers:
1=air,2=N2,3=O2,4=CO2,5=He,6=Ar,7=CO,8=Ne,9=NO,10=N2O,11=SF6,12=Xe,13=CH4\n\r"); return (-1);

        printf("\n\r");

    }

    unsigned char buf[1]={((unsigned char)('9'))};

    num=SendBuf(0,buf,1);

    //error=SendByte(0,(unsigned char)'9');

    fprintf(loggg,"Bytes sent to stop: %d\n",num);

}

else {printf("Syntax error, arg0=0 stops,arg0=1 runs mixture given by the following arguments");return(-1);

}

// _____ CODE _____

//*****closePORT*****

CloseComport(0);

fprintf(loggg,"End communication, port closed\n");

//*****LOG*****

if( loggg){

    if ( fclose( loggg ) )

    {

        printf( "The file 'log_file' was not closed\n" );

    }

}

// All other files are closed:

numclosed = fcloseall();

printf( "Number of files closed by _fcloseall: %u\n", numclosed );

//*****LOG*****

}

```

# Labview pulseoximeter program

